

INFORMATION TO USERS

This manuscript has been reproduced from the microfilm master. UMI films the text directly from the original or copy submitted. Thus, some thesis and dissertation copies are in typewriter face, while others may be from any type of computer printer.

The quality of this reproduction is dependent upon the quality of the copy submitted. Broken or indistinct print, colored or poor quality illustrations and photographs, print bleedthrough, substandard margins, and improper alignment can adversely affect reproduction.

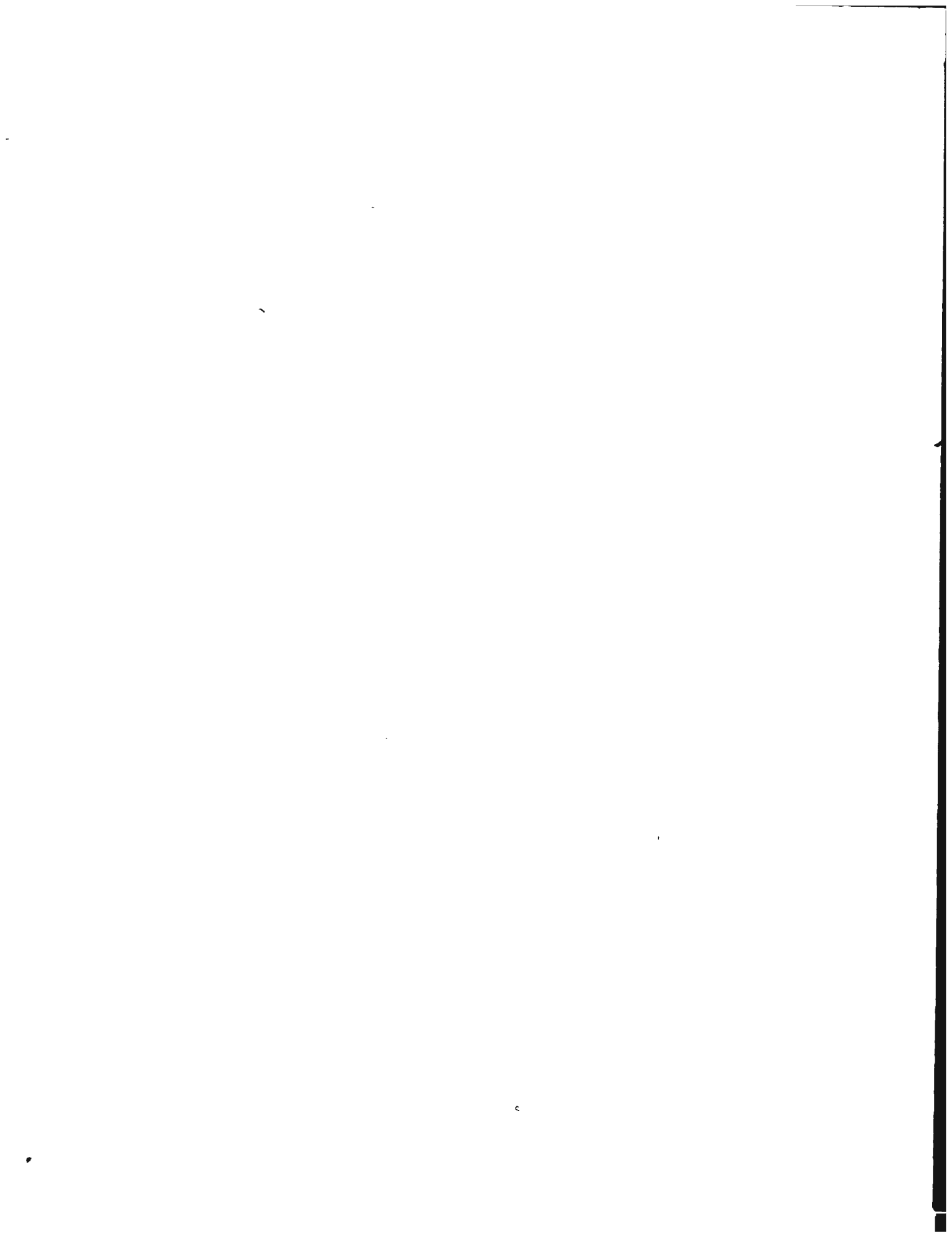
In the unlikely event that the author did not send UMI a complete manuscript and there are missing pages, these will be noted. Also, if unauthorized copyright material had to be removed, a note will indicate the deletion.

Oversize materials (e.g., maps, drawings, charts) are reproduced by sectioning the original, beginning at the upper left-hand corner and continuing from left to right in equal sections with small overlaps. Each original is also photographed in one exposure and is included in reduced form at the back of the book.

Photographs included in the original manuscript have been reproduced xerographically in this copy. Higher quality 6" x 9" black and white photographic prints are available for any photographs or illustrations appearing in this copy for an additional charge. Contact UMI directly to order.

UMI

A Bell & Howell Information Company
300 North Zeeb Road, Ann Arbor, MI 48106-1346 USA
313 761-4700 800 521-0600



UMI Number: 1376670

UMI Microform 1376670

Copyright 1995, by UMI Company. All rights reserved.

This microform edition is protected against unauthorized copying under Title 17, United States Code.

UMI

300 North Zeeb Road
Ann Arbor, MI 48103

UMI Number: 1376670

UMI Microform 1376670


Copyright 1995, by UMI Company. All rights reserved.

This microform edition is protected against unauthorized copying under Title 17, United States Code.

UMI

300 North Zeeb Road
Ann Arbor, MI 48103

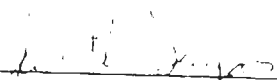
The thesis of Tiangan Lian is approved:



Thesis Advisor



Department Chair



Dean, Graduate School

University of Nevada

Reno

August 1995

ACKNOWLEDGMENT

First all, I like to express my sincere thanks and gratitude to my adviser, Prof Denny Jones, not only for his valuable advisement throughout this thesis work, but also for his friendship and generosity that make myself happy and excited in everyday working with him

My sincere gratitude is extended to Prof Dhanesh Chandra and Prof Liang-Chi Hsu for their supportive attitude and sitting on my examination committee. Thanks to Mr Steve Gill for some literature collection and experiment preparation in the beginning of this project

ABSTRACT

Type 304 stainless steel (304SS) was investigated in simulated swimming pool water and chlorinated NaCl solutions. The effects of chlorination, cyanuric acid and chloride on electrochemical behavior of 304SS was studied with potentiodynamic and cyclic polarization tests, measuring corrosion potential, pitting potentials, and protection potentials. Chlorination showed strong oxidizing ability which significantly increased corrosion potential of 304SS, and increased the susceptibility to pitting and crevice corrosion. Cyanuric acid in chlorinated solution further increased the susceptibility to pitting corrosion, but had no effect on crevice corrosion. Chloride increased pitting corrosion, consistent with previous results in the literature, but this effect was relatively minimal comparing to the effects of chlorination and cyanuric acid. Because of low AFC (available free chlorine) and chloride contents in test solutions, no pitting corrosion was observed on 304SS during 2 month exposure. Corrosion potential of 304SS was decreased by cyanuric acid in general, but was increases by chloride in solutions with presence of both HOCl and cyanuric acid.

TABLE OF CONTENTS

ACKNOWLEDGMENT	ii
ABSTRACT	iii
LIST OF TABLES	vi
LIST OF FIGURES	vii
CHAPTER I	
INTRODUCTION	1
CHAPTER II	
LITERATURE SURVEY AND THEORETICAL APPROACH	6
2 1 General Electrochemistry	6
2 2 Pitting Corrosion	9
<u>Initiation</u>	9
<u>Propagation</u>	12
2 3 Chloride Effect on Pitting	15
2 4 Effect of Dissolved Oxidizer	19
2 5 Corrosion of S S. 304 in Chlorinated Water	22
2 6 The Purpose of This Investigation	25
CHAPTER III	
EXPERIMENTAL PROCEDURES	26
3 1 Specimen Preparation	26

	v
3.2 Solution Preparation	28
3.3 Test Cells	29
3.4 Electrochemical measurements	33
1) Pitting Potentials in simulated pool waters	
without chlorination	33
2) Corrosion Potential Measurements	35
3) Cyclic polarization measurements	36
CHAPTER IV	
RESULTS AND OBSERVATIONS	37
1) Effects of chloride and cyanuric acid	
on pitting susceptibility	37
2) Effects of residual chlorine and chloride	
on corrosion potential, with cyanuric acid	37
3) Effects of residual chlorine and chloride	
on corrosion potential, without cyanuric acid	41
4) Cyclic polarization behavior	48
CHAPTER V	
DISCUSSION	55
CHAPTER VI	
CONCLUSION	61
REFERENCES	63

LIST OF TABLES

<u>TABLE</u>	<u>PAGE</u>
1 Typical swimming pool water chemistry	2
2 Chemical composition of Type 304 stainless steel specimens and filter tank body	27
3 E_{pit} values observed in simulated pool waters without chlorination	39

LIST OF FIGURES

<u>FIGURE</u>	<u>PAGE</u>
1 Influence of pH on the distribution of Cl_2 , HOCl and OCl	3
2 The corrosion rate, i_{corr} , and corrosion potential, E_{corr} , determined by the polarization of anodic and cathodic half-cell reactions	8
3 The critical potentials related with pitting corrosion during cyclic potential scan	11
4 Schematic of processes occurring at a actively growing pit in iron	13
5 Influence of chloride ion concentration on pitting potential and protection potential	17
6 Chloride influence on E_{pit} and E_{prot} measured in 304SS and Ni	18
7 Illustration of corrosion potential changing with increasing exposure time, for an active-passive metal or alloy in oxidizer solution	20
8 Observed shifting of the potentials with exposure time, for alloys in acidified $FeCl_3$ solution	21
9 Two types of corrosion potential fluctuation were observed on 304SS in chlorinated solutions. (a) Micropits formation.	

and (b). Proceeding of crevice corrosion	23
10. Schematic of polarization test cell	30
11. Schematic of corrosion potential test cell	32
12. schematic of computer controlled electrochemical instrumentation	34
13. Effects of chloride and cyanuric acid on pitting potentials	38
14. Effects of HOCl and NaCl on corrosion potentials of 304SS exposed in simulated pool waters containing 50 ppm cyanuric acid	40
15. Effects of HOCl and NaCl on corrosion potentials of 304SS exposed in chlorinated NaCl solutions	42
16. Comparison of corrosion potentials in simulated pool waters to chlorinated NaCl solutions	43
17. The corrosion potentials of 304SS in chlorinated waters containing 10 ppm AFC + 5000 ppm NaCl. Each potential spike represents the procedure of pit initiation and repassivation	45
18. Portion of E_{corr} -T curve showing pit initiation and repassivation	46
19. Corrosion potentials of filter tank and immersed 304SS specimen during 2 month exposure	47
20. HOCl effects on cyclic polarization behavior of 304SS in 2500 ppm NaCl solutions	49

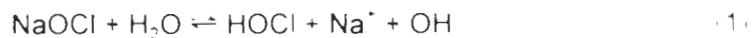
21. HOCl effects on cyclic polarization behavior of 304SS in simulated pool waters, which contain 2500 ppm NaCl + 50 ppm cyanuric acid	50
22 HOCl effects on cyclic polarization behavior of 304SS in 5000 ppm NaCl solutions	51
23 HOCl effects on cyclic polarization behavior of 304SS in simulated pool waters, which contain 5000 ppm NaCl + 50 ppm cyanuric acid	52
24 Comparison of potentials, E_{pit} , E_{prot} , and E_{corr} , determined from cyclic polarization measurements	53

CHAPTER I

INTRODUCTION

Adequate sanitation of swimming pool water is of paramount importance for public safety and health. In the pool and spa industry, chlorination is widely used for water sanitizing. Hypochlorous acid, HOCl, is the stable soluble agent of germicidal power in chlorination. In the USA, there are two chlorination methods commonly used for sanitation of swimming pool water.

Conventionally, sufficient HOCl in pool water is obtained via addition of sodium hypochlorite (NaOCl):



In recent years, electrolytic chlorination devices have been used to produce chlorine (Cl_2) in pool water, which hydrolyses rapidly into HOCl, according to the reaction



The process of producing Cl_2 by electrolytic chlorination device is described as:



Therefore, sufficient dissolved NaCl of 2000-3000 ppm must be maintained in the pool using an electrolytic chlorination device.

Hypochlorous acid (HOCl) is a "weak" acid which partially dissociates as follows.



The dissociation of HOCl is significantly affected by water pH, which is shown in Figure 1.^[2] Hypochlorite is a poor disinfectant compared to hypochlorous acid.^[2] Therefore, an important parameter in pool water chemistry is the chlorine residual or available free chlorine (AFC), which measures hypochlorous acid level in water.

The chlorine products of chlorination form amine and other substances which are either less effective disinfecting agents or irritant to the eyes of swimmers.^[4] Cyanuric acid, $\text{C}_3\text{H}_3\text{N}_3\text{O}_3$, added as a pool water conditioner, stabilizes and maintains chlorine residuals in the presence of sunlight. The typical pool water chemistry can be summarized in Table 1.^[5] These averages vary widely depending on source water chemistry and care in pool water maintenance.

Table 1 Typical swimming pool water chemistry (From the reference [5])

Available free chlorine or AFC, (ppm)	5
Cyanuric acid, (ppm)	50
Sodium chloride, (ppm)	2500
Total alkalinity, (ppm)	100
Calcium hardness, (ppm)	300
Total dissolved solid, (ppm)	1000

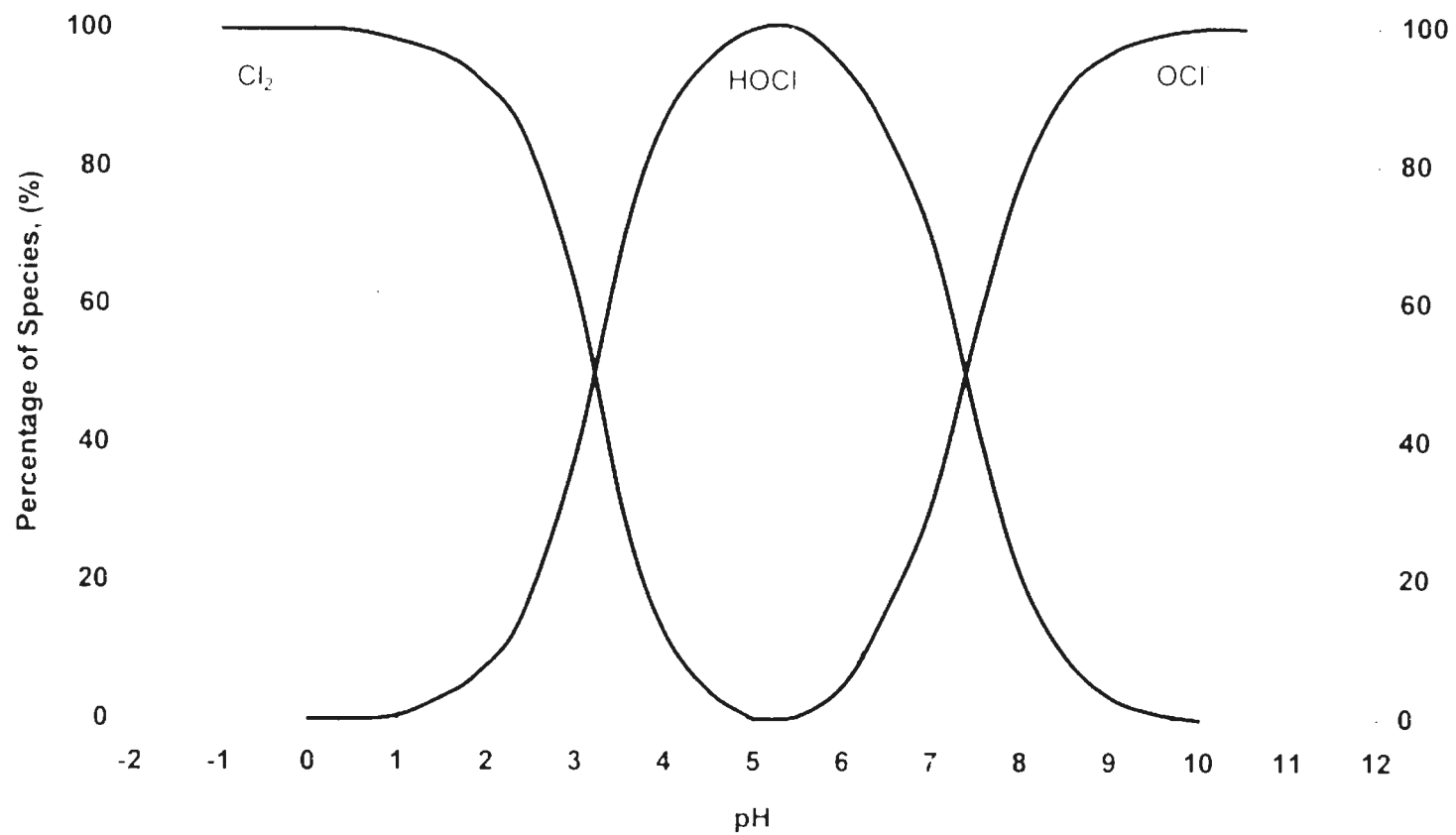


Figure 1 Influence of pH on the distribution of Cl_2 , HOCl and OCl^- (From reference [2])

Type 304 austenitic stainless steel (304SS) is widely used in industry because of its excellent corrosion resistance to many corrosive environments. The addition of 8-10% nickel to iron-18-20% chromium stabilizes the face-centered cubic austenite phase and improves corrosion resistance synergistically with chromium. A thin hydrated, oxidized, chromium-rich passive surface layer on 304SS provides a physical barrier for corrosion resistance. Partial breakdown of passive layer results in localized pitting and crevice corrosion.

Considerable research has been conducted on the corrosion behavior of austenitic stainless steels in chlorinated chloride solutions, often simulating seawater. However, very little work has been reported on corrosion in more dilute domestic water composition, such as used in swimming pools. Contributions of AFC, cyanuric acid and chloride to corrosion of swimming pool equipment are not well understood. This thesis describes research undertaken to determine the interacting effects of residual chlorine, cyanuric acid, and chloride on pitting and corrosion of Type 304 austenitic stainless steel (304SS) in dilute solutions typical of swimming pools in the USA.

Pitting potentials E_{pit} of 304SS were measured in simulated pool waters without HOCl. The measured E_{pit} was used as reference to predict pitting corrosion occurring in the presence of HOCl by raising the potential above E_{pit} with a dissolved oxidizer such as HOCl. Cyclic polarization tests were conducted to

determine the critical pitting potential E_{pit} and protection potential E_{prot} . The comparison of measured E_{pit} and E_{prot} to E_{corr} was used to explain the prediction and observed crevice corrosion. Corrosion potential measurements of 304SS filter tank in chlorinated water showed how HOCl affected the potential of 304SS with time and verified the predictions

CHAPTER II

LITERATURE SURVEY AND THEORETICAL APPROACH

2.1 General electrochemistry

Aqueous corrosion occurs by an electrochemical mechanism in which the overall reaction splits into anodic and cathodic electrode reactions with exchange of electrons. The anodic electrode reaction is the dissolution of metal M to its soluble ion, M^{n+} .



where n is the valence number of M. The accompanying cathodic reaction in a neutral aerated water is the reduction of dissolved oxygen.



The half-cell electrode potentials for the anodic and cathodic reactions are respectively,

$$e_{M/M^{n+}} = e_{M/M^{n+}}^0 - \frac{0.059}{n} \log(M^{n+}) \quad (7)$$

$$e_{O_2/H_2O} = 1.226 - 0.059pH \quad (8)$$

Charge transfer and mass transfer develop two major types of polarization which control the rate of electrochemical corrosion. Polarization reduces the potential difference between anodic and cathodic half-cell electrode potentials while

limiting the reaction rate, which is proportional to current density, I . Anodic and cathodic reactions reach the same potential at the corrosion potential, E_{corr} . The current density at E_{corr} is the corrosion rate, i_{corr} , where anodic and cathodic rates are equal. Figure 2 shows the corrosion rate i_{corr} and corrosion potential E_{corr} determined from polarization curves with interfacial charge transfer control and with mass transfer control.

In chlorinated water, the cathodic processes may include the following reactions ^[6]



$$e_{\text{Cl}_2/\text{Cl}} = 1.395 - 0.0295 \log \frac{(\text{Cl}_2)}{(\text{Cl})^2} \quad (7b)$$



$$e_{\text{HOCl}/\text{Cl}} = 1.494 - 0.0295\text{pH} - 0.0295 \log \frac{(\text{HOCl})}{(\text{Cl})} \quad (8b)$$



$$e_{\text{OCl}^-/\text{Cl}} = 1.715 - 0.059\text{pH} - 0.0295 \log \frac{(\text{OCl}^-)}{(\text{Cl})} \quad (9b)$$

At the same pH, all have higher half cell potentials than the reduction of oxygen (6b). Thus, chlorination lifts the potential of total cathodic reaction, and raises the

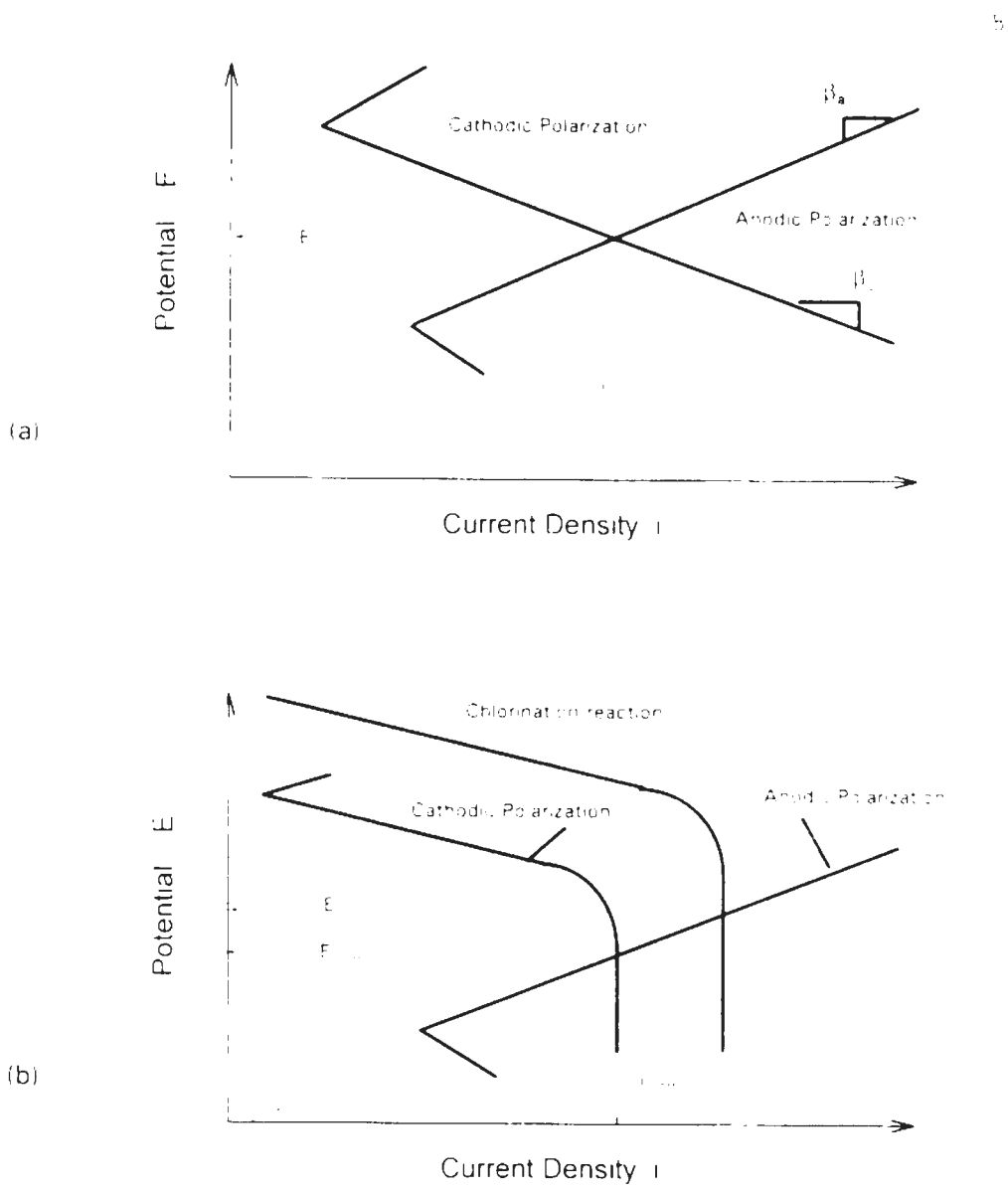


Figure 2. The corrosion rate, i_{corr} , and corrosion potential, E_{corr} , determined by the polarization of anodic and cathodic half-cell reactions, at the situations of (a) Activation polarization control, and (b) concentration polarization control β_a and β_c are the Tafel constants

corrosion potential of the metal in the water to E_{cor} . In Figure 2(b) Ives *et al.*¹⁷ report that chlorination shifted the free-corrosion potential of Au in the noble direction due to the strong oxidizing ability of free chlorine and hypochlorite. Lu and Duquette¹⁸ reported similar potential behavior of 304L stainless steel in chlorinated NaCl solution.

2.2 Pitting Corrosion

Pitting corrosion is a localized attack confined to small areas where the passive surface breaks down locally because of preferential attack by aggressive ions, primarily chloride. Pitting involves two stages: pit initiation after an incubation time, and pit propagation due to the subsequent aggressive local environment developed within the pit.

Initiation Pit initiation is generally difficult to predict. Seemingly identical specimens exposed to the same chemical and electrochemical conditions will pit at variable times and random sites on the surface.^[9]

A passive metal or alloy in contact with an oxidizing solution, in the absence of halide ions, forms an inert surface barrier layer, the passive film, which reduces corrosion rate. However, in an oxidizing solution containing chloride ions, the normally protective passive film breaks down locally, initiating pitting and crevice corrosion.

The critical pitting potential, E_{pit} , measures the susceptibility to pitting corrosion. It is the potential above which drastically increased current density indicates pit initiation. Figure 3 shows a schematic anodic polarization scan in which pits initiate when the linearly increasing potential reaches the pitting potential, E_{pit} . The actual mechanism of pit initiation at E_{pit} is not well understood. Pits initiate at flaws, pores, or other physical defects in the film^[10]. When potential approached E_{pit} , Wilde^[11] measured increased surface Cl⁻ concentration with Cl⁻ sensitive microelectrodes.

Czachor *et al.*^[12] observed that small islands of chloride salt formed on the metal surface, even though the metal surface was pit free at potential 60 mV more active than E_{pit} . In a similar manner, Okada^[13] stressed that pitting starts when sufficient chloride ions adsorb on the passive film to form a transitional complex with a lattice cation at the film-solution interface. The pitting potential can be regarded as the potential, at which Cl⁻ ions accumulate enough to start the metal dissolution at weak spots^[14]. For a particular alloy, the critical pitting potential is known to be a function of the nature and concentration of the aggressive ion as well as the temperature^[15].

The increase in anodic current above E_{pit} represents the polarization for the new anodic process characteristic of the pit environment. The experimental value of E_{pit} depends very much on procedure. The characteristic pitting potentials vary according to the method of measurement, and particularly the potential scan rate

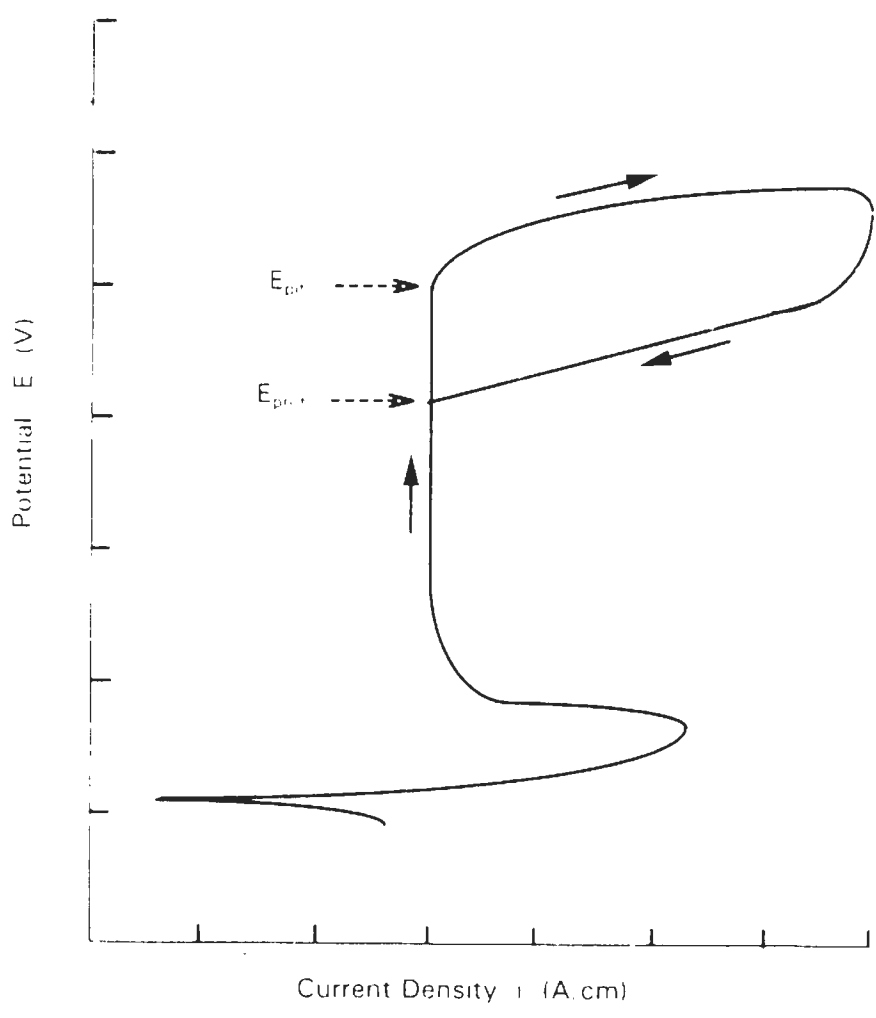
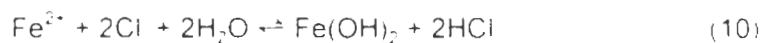


Figure 3 Critical potentials related with pitting corrosion during cyclic potential scan

Rapid potential scanning elevates E_{pit} . Slow scanning allows more time for chloride accumulation and pit initiation, and lowers E_{pit} .^[16]

Propagation In the early stage of pit development, the weak spots in the passive film attract Cl^- ions, which are unevenly distributed on metal surface, even though potential is practically uniform. Under these conditions, the dissolution of metal occurs at the weak spots in the passive film where Cl^- ions have accumulated, but the rest of metal surface with little adsorption of Cl^- ions maintains the passive state.^[17]

Once a pit initiates, the electrochemical reactions within the pit dominate the pit growth. Jones^[18] has graphically depicted the self-propagation or autocatalytic mechanism of pit growth in Figure 4. For pitting of carbon steel or iron in a slightly alkaline chloride solution, copious anodic production of positively charged Fe^{2+} at the initiation site attracts negative anions, e.g., Cl^- . Hydrolysis by



produces local pH reductions at the initiation site, because reaction product HCl is a strong acid. The acid chloride and low pH further accelerate anodic dissolution, which in turn further catalyzes the growth of pit. $\text{Fe}(\text{OH})_2$ precipitates at the pit mouth and forms insoluble cap when outward diffusing Fe^{2+} from the pit interior is oxidized to Fe^{3+} . The cap impedes easy escape of Fe^{2+} but is sufficiently porous to

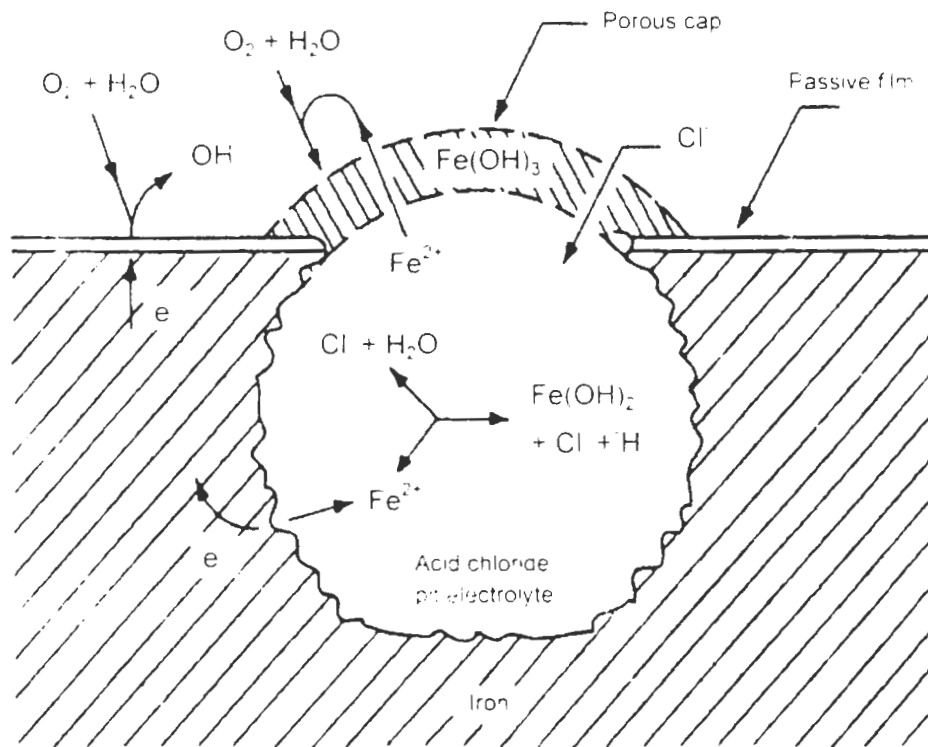


Figure 4. Schematic of processes occurring at an actively growing pit in iron. (From reference [18].)

permit migration of Cl^- to the pit, thereby sustaining a high acid chloride concentration in the pit. The coupling of the passive bulk surface with the active interior drives the anodic dissolution within the pit.

Most mechanistic models for pit propagation are based on the assumptions that the anodic reaction occurs only within the pit and cathodic reactions occur only on the boldly exposed surface. To simplify the models, the pit walls are assumed to be unreactive. The propagation of these models are based on mass transport in which the rate of pit propagation is controlled by transport of corrosion products out of the pit. However, Beavers and Thompson^[19] reported that the propagation behaviors of nonreactive wall and reactive wall in artificial pits were significantly different. For the pits with nonreactive wall, relatively high rate of anodic dissolution on pit base results deep pits because of the coupling effect of the boldly exposed surface. On the other hand, for the pits with reactive wall, the high rate of anodic dissolution on the region near the pit mouth produces shallow pits. These models may provide some help in relating the kinetics of pit growth with pit morphology though the authors did not relate the models to the real pit situation.

Smialowska^[20] summarized that the rate of pit growth depended on the following parameters

- Concentration of chloride ions in the solution
- Presence of nonaggressive anions in the solution
- Temperature

- Potential
- Properties of the passive film
- Crystal orientation of the metal grain on which pitting occurs

All of the above parameters exert some influence on the composition of the electrolyte within pits, and can therefore affect the rate of pit growth

Even after the potential is lowered below E_{pit} , the interior of a growing pit is still in the active state with high dissolution rate. Thus, pits are repassivated only when potential is below the protection potential E_{prot} , as shown in Figure 3. Any potential active to E_{pit} , which is the open-circuit-anode potential of pit interior, will cathodically polarize the pit interior and suppress or stop corrosion within the pits.

Pits grow only at potentials more noble than the E_{pit} . As is E_{pit} , E_{prot} is very much a function of experimental procedure. Longer time above E_{pit} , or slower potential scan, allows greater chloride concentration within the pits. As pointed out by Wilde,^[22] protection potential E_{prot} measurements are related only to the conditions necessary to repassivate a growing pit after a specific period of propagation. Protection potential E_{prot} is not a unique material property, and it varies in magnitude with the experimental conditions used to measure it.

2.3 Chloride effect on pitting potential

The chloride ion is the most aggressive pitting agent and the most thoroughly studied because of its wide distribution in nature. With high concentration of chloride

ions, the passive film on a susceptible metal to pitting suffers local damage, while low concentrations produce only an increase of the anodic current in the passivity range^[23]

Increasing Cl⁻ concentration usually shifts pitting potential E_p , in the active direction for most alloys, as well as carbon steels. The dependence of pitting potential E_{pit} on chloride ion concentration follows a simple relationship in equation (11)^[23]

$$E_p = A - B \log[Cl^-] \quad (11)$$

where A and B are constants dependent on various factors, such as the composition of electrolyte, the measurement technique, and properties of the metal. The similar relationship between protection potential E_{prot} and Cl⁻ concentration was observed in carbon steel by Ergun and Turan^[24] as well. Figure 5 shows their experimental results of the influence of chloride ion concentration on the pitting potential and protection potential of carbon steel, in K₂CO₃ solution and sodium benzoate solution^[24]. The effect of increasing Cl⁻ concentration in neutral NaCl solution is to shift E_{pit} in the active direction by about 0.09 V for a 10-fold change in concentration. Similar behavior on E_{pit} of Type 304 stainless steel was observed by Leckie and Uhlig,^[25] shown in Figure 6, as well by Johnson^[26]. However, the Cl⁻ effect on E_{prot} of 304SS is rarely reported in the literature. For some metals or alloys, E_{prot} can be independent of Cl⁻ concentration, as reported by Sussek and

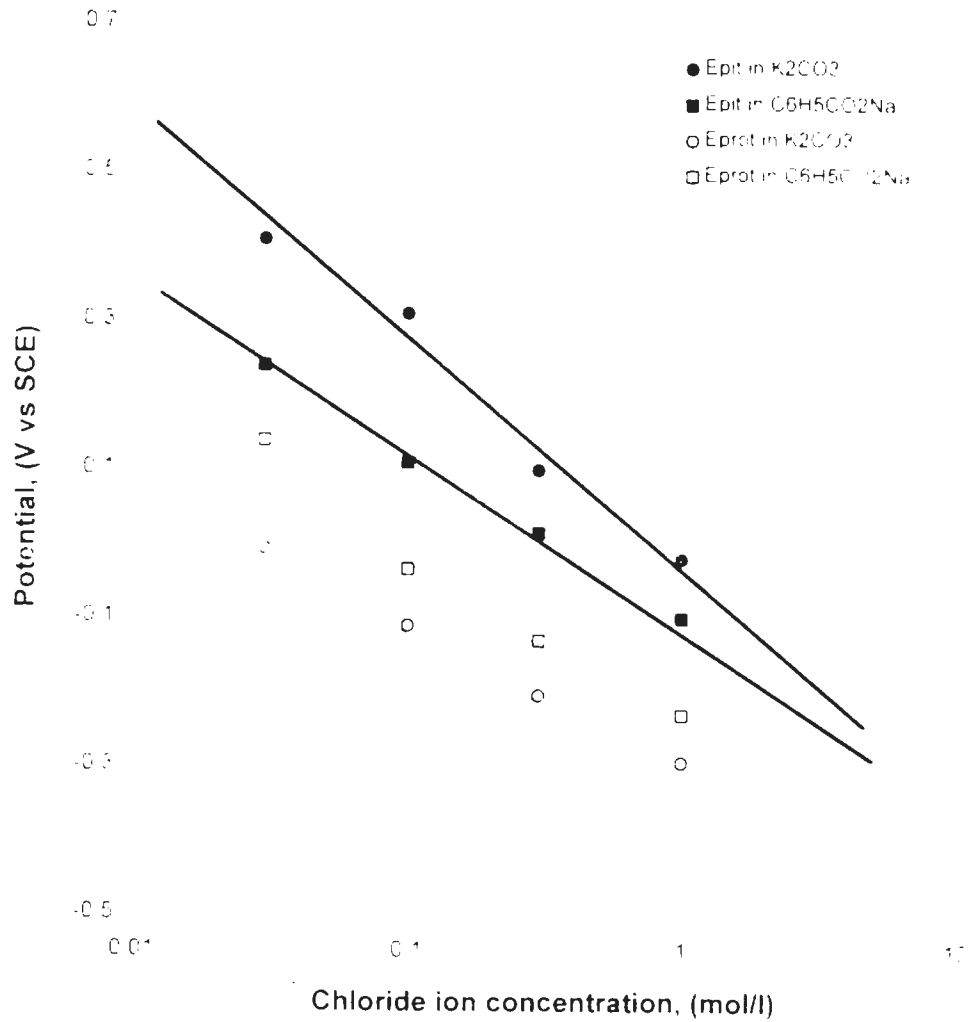


Figure 5. Influence of chloride ion concentration on pitting potential and protection potential of carbon steel. (From reference [24].)

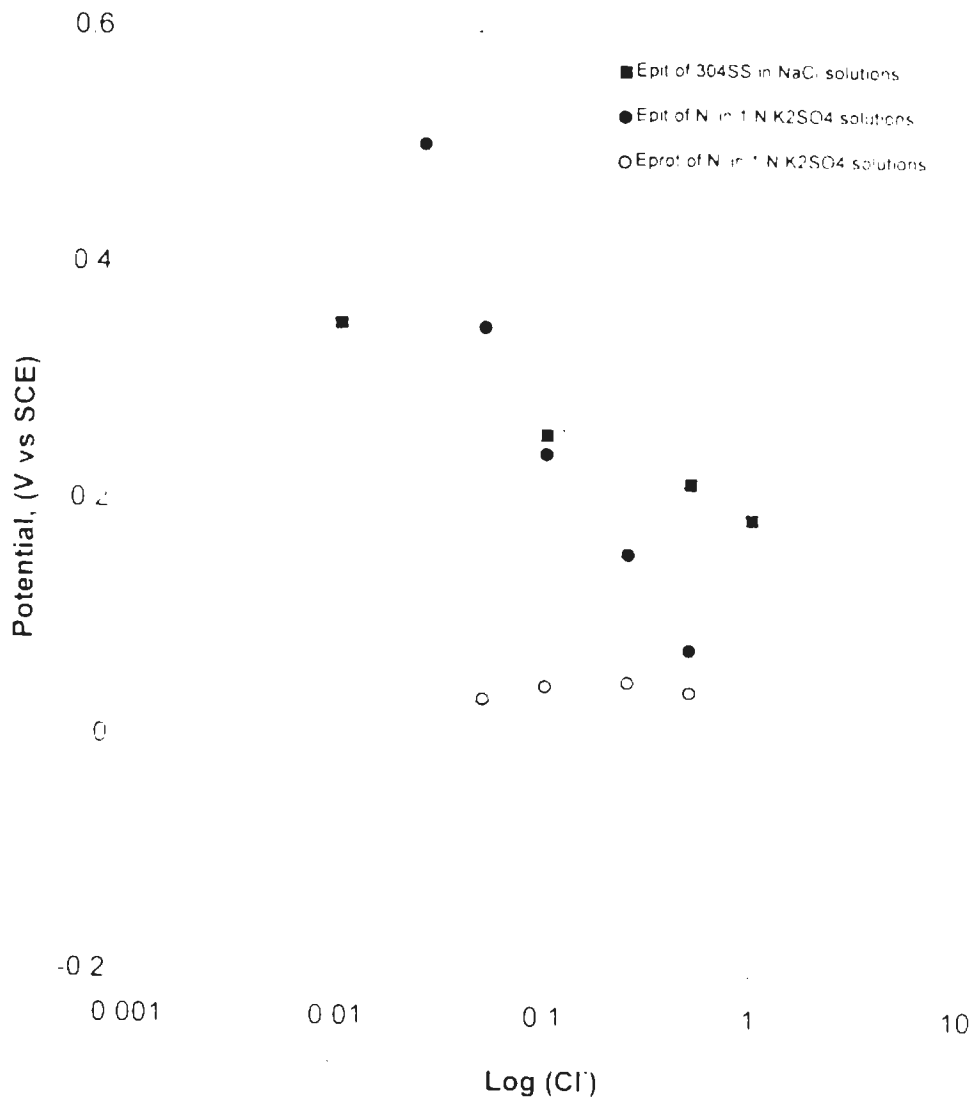


Figure 6. Chloride effects on 1) pitting potential of 304SS in NaCl solutions, (From reference [25]), and 2) pitting and protection potentials of Ni in 1 N K_2SO_4 solution, (From reference [27])

Kesten^[27] in their studies of Cl⁻ effects on characteristic pitting potentials of Ni, as shown in Figure 6

2.4 Effect of Dissolved Oxidize.

Addition of a stronger oxidizer increases the driving force for corrosion. As described in section 2.1, the presence of a more noble half-cell potential increases the corrosion potential in the noble direction. For active-passive alloys, such as austenitic stainless steels, increasing corrosion potential can induce passivity and significantly reduce the corrosion rate. However, further increase of corrosion potential can cause pitting corrosion when the corrosion potential exceeds E_{pit} .

Long term exposure in an oxidizing solution can enhance the corrosion potential and induce the initiation of pitting, even though a metal or alloy is initially in passive state with the corrosion potential below E_{pit} . The passive current density i_{pass} decreases and the corrosion potential becomes more noble with time as the passive film thickens, as shown in Figure 7^[28]. The anodic polarization curve moves to the left with exposure time, assuming no change in E_{pit} . After a critical exposure time, when the corrosion potential reaches E_{pit} , pitting corrosion can begin. This theory explains potential measurements on corrosion resistant alloys during exposure in acidified $FeCl_3$ solution, as reported by Wilde and Williams,^[29] and shown in Figure 8. The corrosion potential increases during early stages of exposure. Some time after potential reaches E_{pit} , a marked drop is followed by a

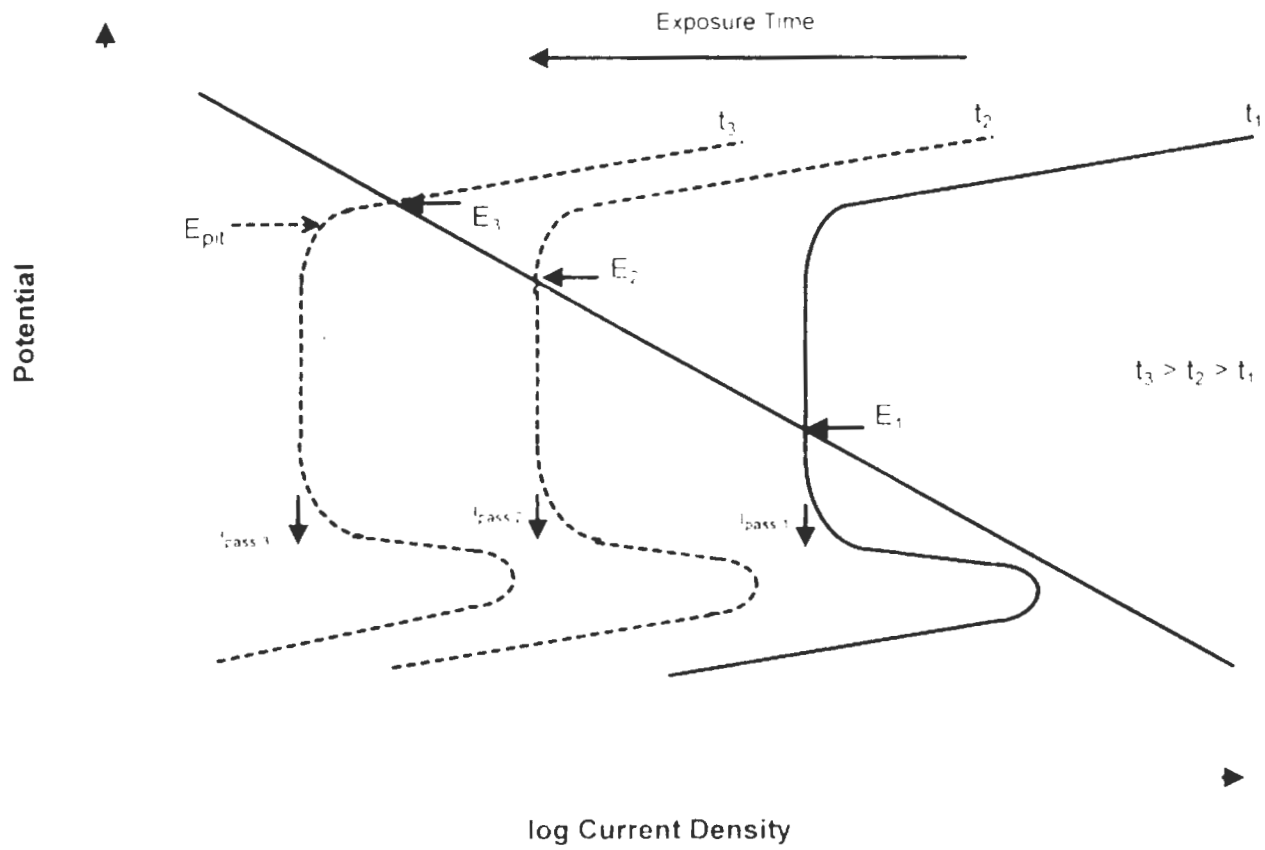


Figure 7 Illustration of corrosion potential changing with increasing exposure time, for an active-passive metal or alloy in oxidizer solution.

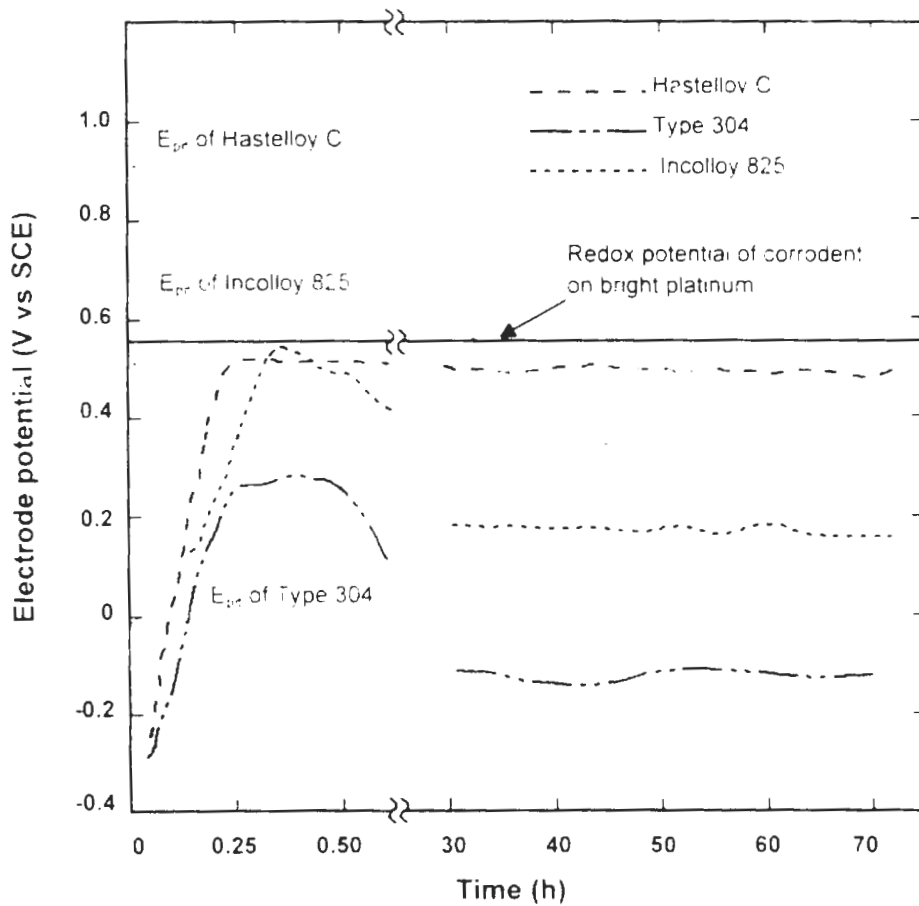


Figure 8. Corrosion potential measurements on corrosion resistant alloys during pitting in acidified FeCl_3 solutions (1.185 N in Cl). (From reference [29].)

stable corrosion potential with pitting at an active level

For Type 904L stainless steel (UNS N08904) in natural seawater^[31] chlorination shifted the free-corrosion potential in the noble direction because of the strong oxidizing ability of residual chlorine. More noble potentials increased the pitting tendency and stimulated pit growth. Lu and co-workers^[31] studied the electrochemical conditions within growing pits formed on Type 301 stainless steel in chlorinated solution of 300 ppm HOCl + 0.6 M NaCl + 0.1 M Na₂SO₄. The study revealed that strong oxidizing ability of free chlorine raised the mixed potential on surrounding surface, and increased the potential difference between the active region of localized attack and the adjacent surface. The presence of HOCl accelerated the pitting corrosion.

2.5 Corrosion of 304SS in chlorinated water

The corrosion behavior of 304SS has been studied in chlorinated water with high chlorine concentration levels. Magaino *et al.*^[32] studied the fluctuation of corrosion potential of Type 304 stainless steel immersed in 2 M NaCl + 0.1 M NaOCl aqueous solutions. Formation and repassivation of micropits were indicated by a rapid drop followed by a slow potential increase, as shown in Figure 9(a). For crevice corrosion, the corrosion potential dropped drastically after about 2.5 hour of immersion, and continued to decrease slowly thereafter, as shown in Figure 9(b).

Daufin and co-workers^[33] observed pitting initiation on several stainless steels

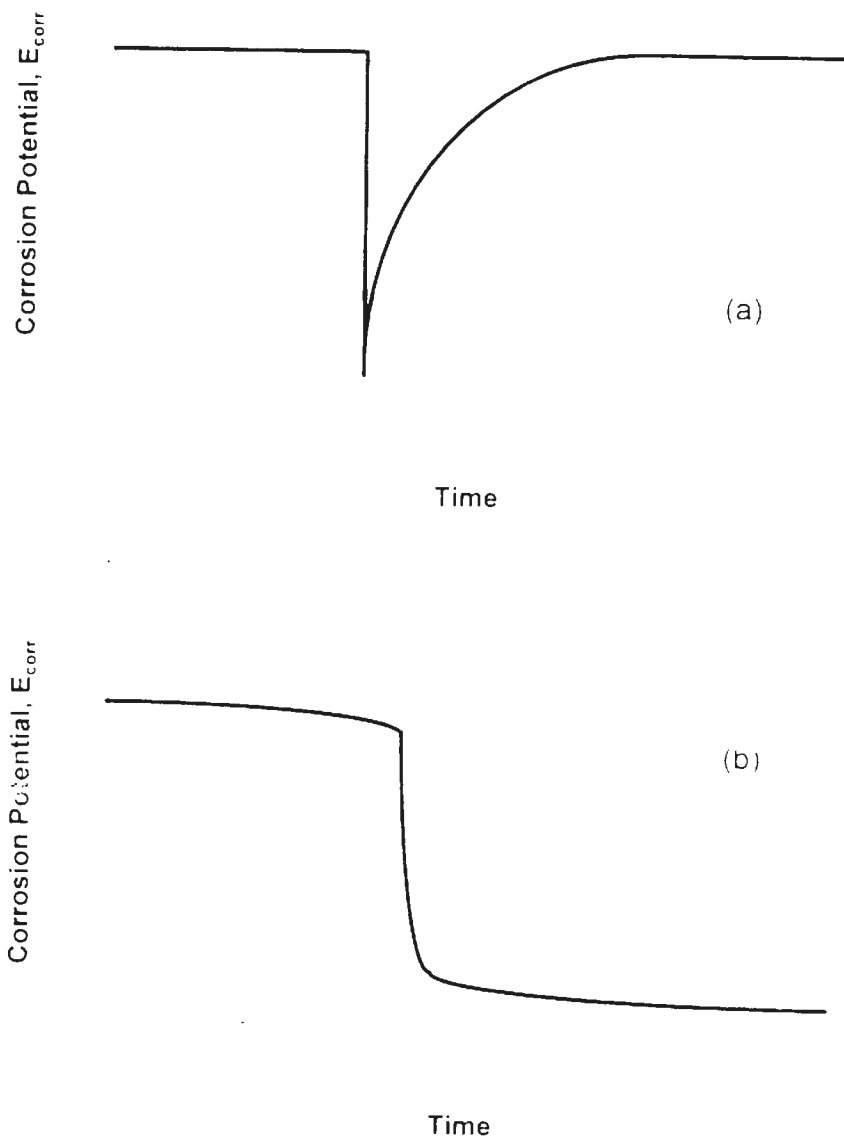


Figure 9. Two types of corrosion potential fluctuation were observed on 304SS in chlorinated solutions. (a). Micropits formation and repassivation; (b). Proceeding of crevice corrosion. (From reference 32)

in contact with an oxidizing chlorite solution (2.5 M NaCl + 4 M NaOCl) at 70°C. Repassivation of not propagating pits and activation of continuously growing pits were observed on 50 cm² specimen area. The initiation of both pit types depended not only on the alloy potential, but also on the duration of contact with the solution. After a rapid continuous potential rise from the immersion potential (about -200 mV vs SCE), fluctuations appeared as rapid drops followed by a slower increase characteristic of repassivated pits. After some time above the pitting potential E_{pit} (around 370 mV vs SCE) a significant potential drop (>100 mV) eventually occurred and active pits were observed. Repassivation of active fluctuations produced no active pits or any other visible attack.

Yoshii *et al.*^[4] found the pitting corrosion of 304SS in chlorinated NaCl solutions became more pronounced with increasing Cl⁻ concentration (50 - 1000 ppm), residual chlorine (0 - 10 ppm), and temperature (40°C - boiling point). However, Lu and Duquette^[8] observed that chlorination up to 180 ppm AFC not only increased corrosion potential of 304SS, but also raised pitting and protection potentials in 0.5 M NaCl solution. The increase on E_{pit} and E_{pro} suggests enhanced resistance to pitting initiation, and accelerated propagation on pitting or crevice corrosion.

The above studies had much higher residual chlorine levels or temperature in test solutions than swimming pool water. However, specific studies on corrosion of Type 304 stainless steel in actual or simulated swimming pool waters are rare.

In addition, swimming pool water often contains cyanuric acid, which is an inhibitor to oxidizing ability of HOCl. Therefore, corrosion behavior of S S 304 in swimming pools might differ from what has been reported for typical chlorinated solutions.

2.6 The purpose of this investigation

The purpose of this investigation can be itemized as followings

- 1) Study the pitting susceptibility of Type 304 austenitic stainless steel in simulated swimming pool water.
- 2) Study how chlorination affects the electrochemical properties of 304SS in pool water.
- 3) Study how cyanuric acid influences corrosion behavior due to its inhibition against oxidizing power of HOCl.
- 4) Explain observed phenomenon in this investigation.

CHAPTER III

EXPERIMENTAL PROCEDURES

DC electrochemical polarization methods were used to investigate the localized corrosion behavior of Type 304 stainless steel in simulated swimming pool water. Somewhat higher concentrations of water chemistry were included to anticipate potentially harsh conditions observed occasionally in service. The investigation pursued its objectives through following paths:

- 1) Measure susceptibility to localized corrosion from critical pitting and protection potential determinations, as a function of water chemistry using anodic polarization as a convenient substitute for dissolved oxidizers.
- 2) Monitor corrosion potential in the presence of chlorination, a dissolved oxidizer in swimming pools, and correlate corrosion potential fluctuations near the critical potentials with initiation and growth of localized corrosion.
- 3) Compare the electrochemical behavior in varied water chemistries to reveal how significantly the solute species, such as available free chlorine, chloride, and cyanuric acid affect localized corrosion in pool water.

3.1 Specimen Preparation

Type 304 austenitic stainless steel materials were received from three sources listed in Table 2 along with chemical compositions given by Metal Analysis

Table 4. Chemical composition of Type 304 stainless steel specimens and filter tank body (element contents in weight %)

Source	C	Mn	Si	P	S	Cr	Ni	Mo	Fe
Hardware manufacture	0.03	1.89	0.38	0.022	0.005	18.48	8.15	0.37	Bal
Commercially purchased	0.06	1.94	0.32	0.021	0.006	18.43	9.11	0.36	Bal
Pool filter case	0.04	1.23	0.43	0.028	0.005	17.51	9.65	0.45	Bal

Inc., Huntington park, CA. The 304SS specimens were received from the first two sources as coupons cut from cold rolled, mill annealed sheet. They were tested in the as-received condition to more closely simulate the metallurgical condition of the filter tank, which was tested to study effects of large surface area in a functioning hardware component.

Kreep Krauly USA, Inc., Sunrise, FL, provided a number of 304SS coupons from their vendors for initial experiments. These 304SS coupons had the dimensions of 18.75 mm × 100 mm × 1.6 mm (3/4" × 4" × 1/16"). Additional 304SS coupon specimens were later purchased from Pacific Sensor Co., Fountain Valley, CA. They had dimensions of 18.75 mm × 150 mm × 0.625 mm (3/4" × 6" × 0.025").

Each test specimen was manually ground to a 600 grit surface finish on all faces, degreased with acetone, rinsed consecutively in tap water and distilled water, and dried. A specimen was immersed in the test solution for subsequent electrochemical measurements immediately after surface preparation. Some specimens, which were tested for anodic polarization behavior, were covered with PVC tape so that only an area of 1 × 1 cm² was exposed. The inner surface of the filter tank was abraded to a 600 grit surface finish, then rinsed consecutively in tap water and distilled water.

3.2 Solution Preparation

Two similar solution types were used in this investigation: simulated swimming

pool water and chlorinated NaCl solution

1) Simulated swimming pool water. Typical swimming pool water chemistry is listed in Table 1^[5]. The chemistry was selected between the high and low extremes of the typical values^[5]. Residual chlorine, cyanuric acid, and chloride were added to a base water of 100 ppm total alkalinity and 300 ppm calcium hardness at ambient temperature. Reagent grade NaHCO_3 was used to adjust the alkalinity, and CaCl_2 , commercially available as Guarder calcium hardness increaser, (Hydrotech Chemical Co., Decatur, GA), was added to adjust the hardness in base water.

2) Chlorinated NaCl solution. Reagent grade NaCl was dissolved in distilled water to obtain the NaCl concentrations of 2500 and 5000 ppm with no alkalinity or hardness adjustments. Sodium hypochlorite (NaOCl) was added in order to obtain the residual chlorine level.

Taylor K-2005 DPD colorimetric^[35] chlorine test kit (Taylor Technologies, Inc., Sparks, MD), was used to measure available free chlorine (AFC) in all solutions.

3.3 Test cells

Three types of test cells were used in this investigation: a) polarization test cell, b) corrosion potential test cell, and c) filter tank cell.

a) The polarization cell (Figure 10) was used for anodic polarization and cyclic polarization tests, and for some continuous corrosion potential measurements as well. It consisted of a glass flask with a Teflon lid. Holes in the lid located the

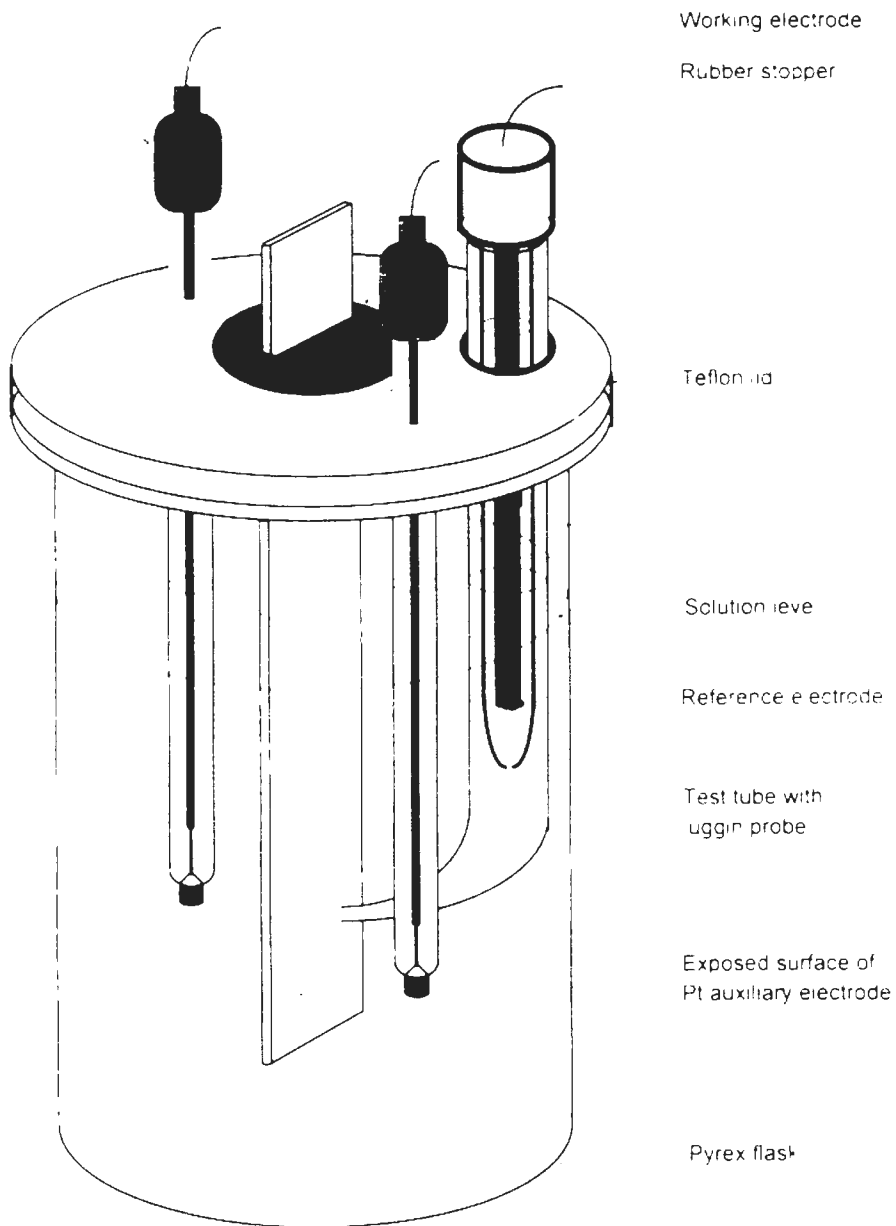


Figure 10. Schematic of polarization test cell.

electrodes and additional necessary entry ports. The specimen working electrode, held by a polytetrafluoroethylene (PTFE) coated rubber stopper, was located in the center of cell with a pair of Ingold Pt-805 platinum auxiliary electrodes (Ingold Electrodes Inc., Wilmington, MA) on either side. A glass tube, with the Luggin probe approaching the working electrode, electrolytically connected the saturated calomel reference electrode (SCE) with the working electrode.

b) The corrosion potential test cell (Figure 11) was used to measure corrosion potential during long exposures. The specimen was inserted into the test solution through a slit cut in the cap center of the 1-liter polyethylene plastic jar used as the container. The usual hole in the cap allowed easy access for the SCE reference electrode.

c) The filter-tank cell was formed by filling the test solution into the cylindrical filter tank of 45 cm (or 18 inch) diameter, 75 cm (or 30 inch) height, and capacity of 75 liters (20 gallons). The inner tank surfaces served as the working electrode. A movable plastic tube with Luggin probe containing a SCE reference electrode was used to measure the potential of selected positions on the inner tank surface. Potentials were measured vertically along the longitudinal seam weld of the tank and again vertically on the tank body, 90° from the first group but not along a welding line. Two outlets located on the bottom of tank, plugged by rubber stoppers, formed crevices in the cell.

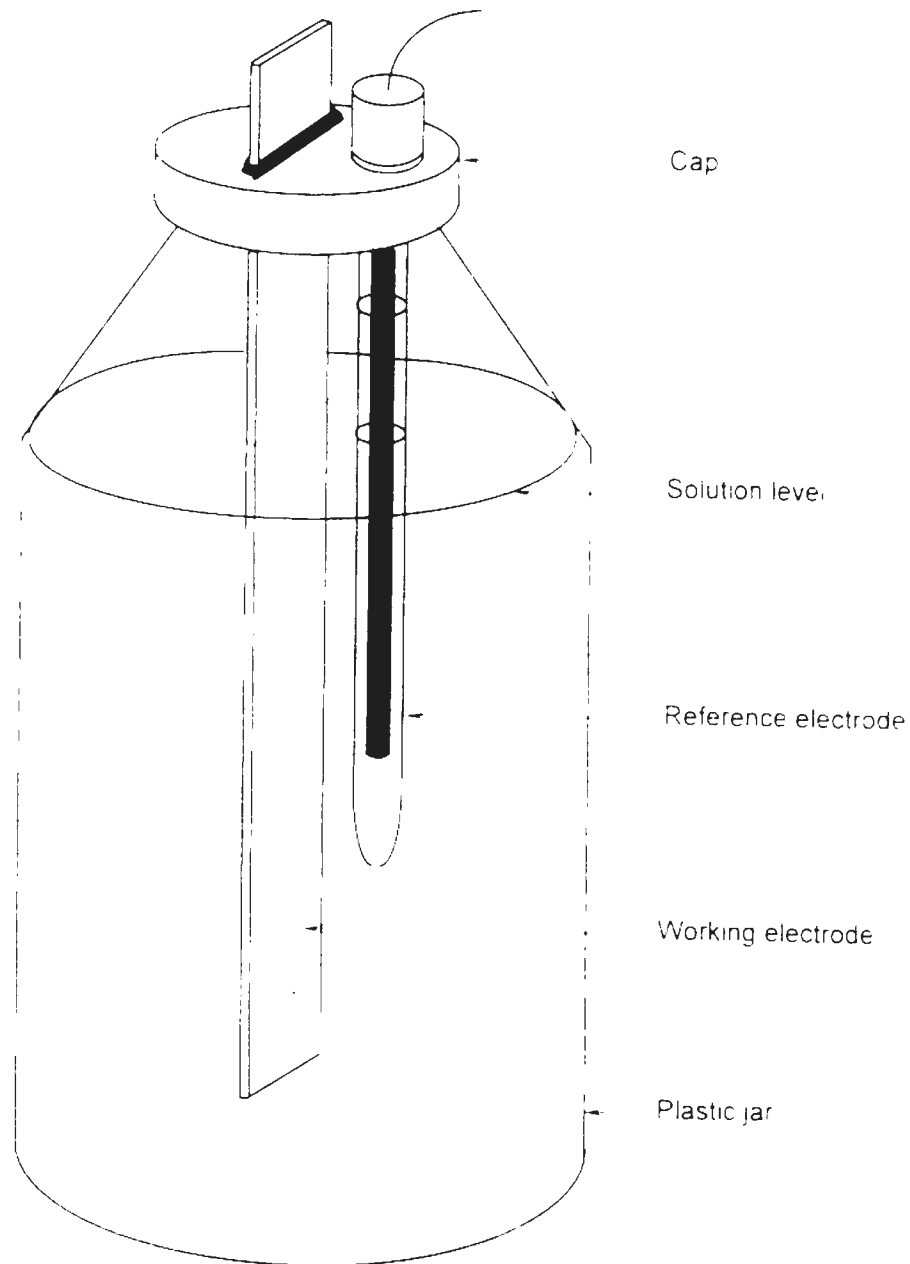


Figure 11. Schematic of corrosion potential test cell.

3.4 Electrochemical measurements

Electrochemical DC polarization tests were conducted with a computer-controlled electrochemical work station, consisting of an IBM compatible 386 computer loaded with potentiostat and software CMS100. (from Gammy Instruments, Inc., Willow Grove, PA) Figure 12 shows the instrument schematic for electrochemical experiments. The auxiliary electrodes were not necessary for the tests in immersion test cell and filter tank cell.

1) Pitting potential in simulated pool waters without chlorination

Pitting potential measurements were conducted in a base water containing 100 ppm total alkalinity (adjusted with reagent grade NaHCO_3) and 300 ppm calcium hardness (adjusted with CaCl_2 , Guarder calcium hardness increaser, Hydrotech Chemical Co., Decatur, GA). To the base water were added reagent-grade NaCl at 0, 1000, 2000, 2500, 3000, and 5000 ppm in various combinations with commercial-grade cyanuric acid (Guardex conditioner, Hydrotech Chemical Co., Decatur, GA) at 0, 25, 50, 75, and 100 ppm.

The potentiodynamic method was used to observe the pitting potential E_{pit} , following ASTM Standard G-5^[36] in the cell of Figure 10. After one hour immersion, the potential scan started anodically from a potential 60 mV active to $E_{\text{c.o.c.}}$ and stopped when the anodic current density reached 1 mA/cm^2 . The exposure area on working electrode surface was 1 cm^2 . Potential scan rate was 600 mV/hr. The

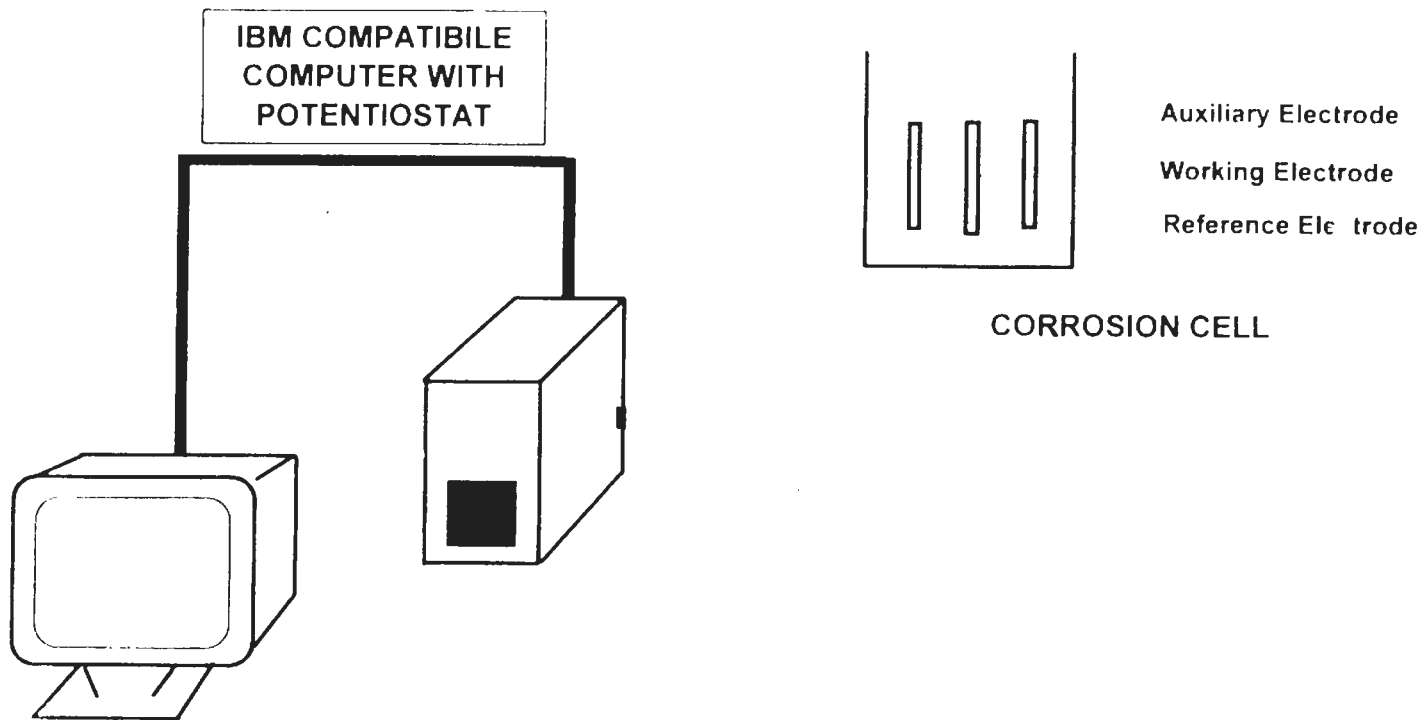


Figure 12 Schematic of computer controlled electrochemical instrumentation

results were recorded automatically, and plotted as the potential versus log current density polarization curve by the computer software. Values of critical pitting potential E_{pit} were obtained by computer analysis of the polarization curve.

2) Corrosion potential measurements.

Simulated pool waters had fixed 50 ppm cyanuric acid, residual chlorine at 0, 5, 10 and 30 ppm, and NaCl at 2500 ppm and 5000 ppm. Residual free chlorine was adjusted with reagent grade sodium hypochlorite (NaOCl) and monitored as ppm AFC with the Taylor K-2005 DPD colorimetric chlorine test kit (Taylor Technologies, Inc., Sparks, MD). Each of eight plastic jars contained one of the above eight combinations. Chlorinated NaCl solutions were arranged in eight plastic jars as well, according to the combinations of AFC at 0, 5, 10 and 30 ppm with NaCl at 2500 and 5000 ppm. The exposure area of specimen was 35 cm². Corrosion potential was recorded continuously or three times every day.

Corrosion potentials were recorded once a day in the filter tank filled with chlorinated water of 10 ppm AFC + 5000 ppm NaCl. Continuous measurement of corrosion potential was conducted in the polarization test cell where the specimen, with 35 cm² exposure area, was exposed in 10 ppm AFC + 5000 ppm NaCl solution for several weeks. Continuous measurements were interrupted three times a day, in order to measure the potentials in corrosion potential test cells and in filter tank.

3) Cyclic polarization measurement.

The cyclic polarization curve provided potentials for pit initiation, E_{pit} , and pit repassivation, E_{prot} . By comparison to E_{corr} from immersion test, the observed E_p and E_{prot} indicated if localized corrosion would occur on a specimen during the long term exposure in chlorinated water. The technique of cyclic polarization measurement in this research was based on the ASTM Standard G-61,^[37] but the maximum anodic current density for starting reverse scan was chosen at 1 mA/cm^2 (about 35 mA), instead of 5 mA/cm^2 in standard, to assure enough current supplied by power source. The exposure area of the working electrode was 35 cm^2 . Eight solutions were used for the cyclic polarization tests: simulated pool waters with Calcium hardness and alkalinity consisting of AFC at 0 or 10 ppm in combination with NaCl at 2500 or 5000 ppm, NaCl solutions consisting of NaCl at 2500 or 5000 ppm in combination with AFC at 0 or 10 ppm.

CHAPTER IV

RESULTS AND OBSERVATIONS

The results and observations are presented in four sections: 1) Effects of chloride and cyanuric acid on pitting susceptibility, 2) Effects of residual chlorine and chloride on corrosion potential, with presence of cyanuric acid, 3) Effects of residual chlorine and chloride on corrosion potential, without presence of cyanuric acid, and 4) Cyclic polarization behavior.

1) Effects of chloride and cyanuric acid on pitting susceptibility.

Table 3 lists the E_{pit} values in each water composition, including 100 ppm total alkalinity and 300 ppm calcium hardness. The E_{pit} values are plotted versus chloride concentration in Figure 13. Pitting potentials decreased consistently with increasing chloride content in simulated pool water without residual chlorine. Cyanuric acid showed inconsistent effects on pitting potential. At 0 and 1000 ppm NaCl, cyanuric acid from 0 to 100 ppm decreased pitting potential. Above 1000 ppm NaCl, E_{pit} still decreased but not in regular order with increasing cyanuric acid.

2) Effects of residual chlorine and chloride on corrosion potential with cyanuric acid

The corrosion potentials versus exposure time were measured in simulated

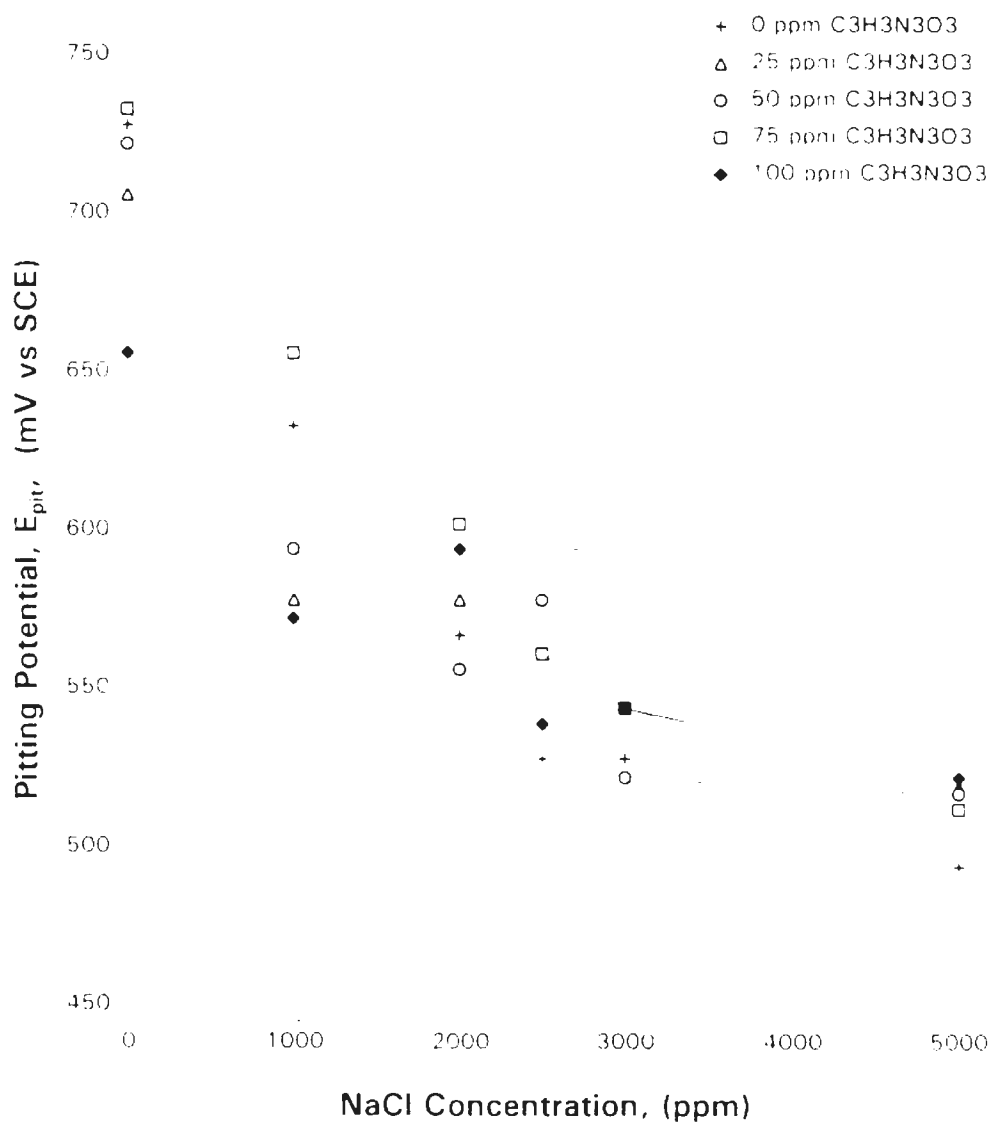


Figure 13. Effects of chloride and cyanuric acid (C₃H₃N₃O₃) on pitting potential, E_{pit} , in simulated pool water containing 100 ppm total alkalinity and 300 ppm calcium hardness.

Table 3: E_{pit} (in mV vs SCE) values observed simulated pool waters without chlorination

Sodium chloride (ppm)	Cyanuric acid (ppm)				
	0	25	50	75	100
0	728	706	722	733	656
1000	633	578	594	656	572
2000	567	578	556	602	594
2500	528	561	578	561	539
3000	528	544	522	544	544
5000	494	519	517	512	522

pool waters, containing constant 50 ppm cyanuric acid, and variable chlorine 2 residual and NaCl contents. Figure 14 shows the change of corrosion potentials during 50 day immersions.

Without chlorine residual, the corrosion potentials in the waters with 2500 ppm and 5000 ppm NaCl show nearly same measurement and tendency. In first 7 days, the potentials reach a maximum value at -50 mV, then drift active to a stable value at about -120 mV. With available free chlorine, the corrosion potentials move continuously in noble direction, and reach a plateau after about 20 days. At 5 ppm AFC, there was little difference between 2500 and 5000 ppm NaCl on corrosion

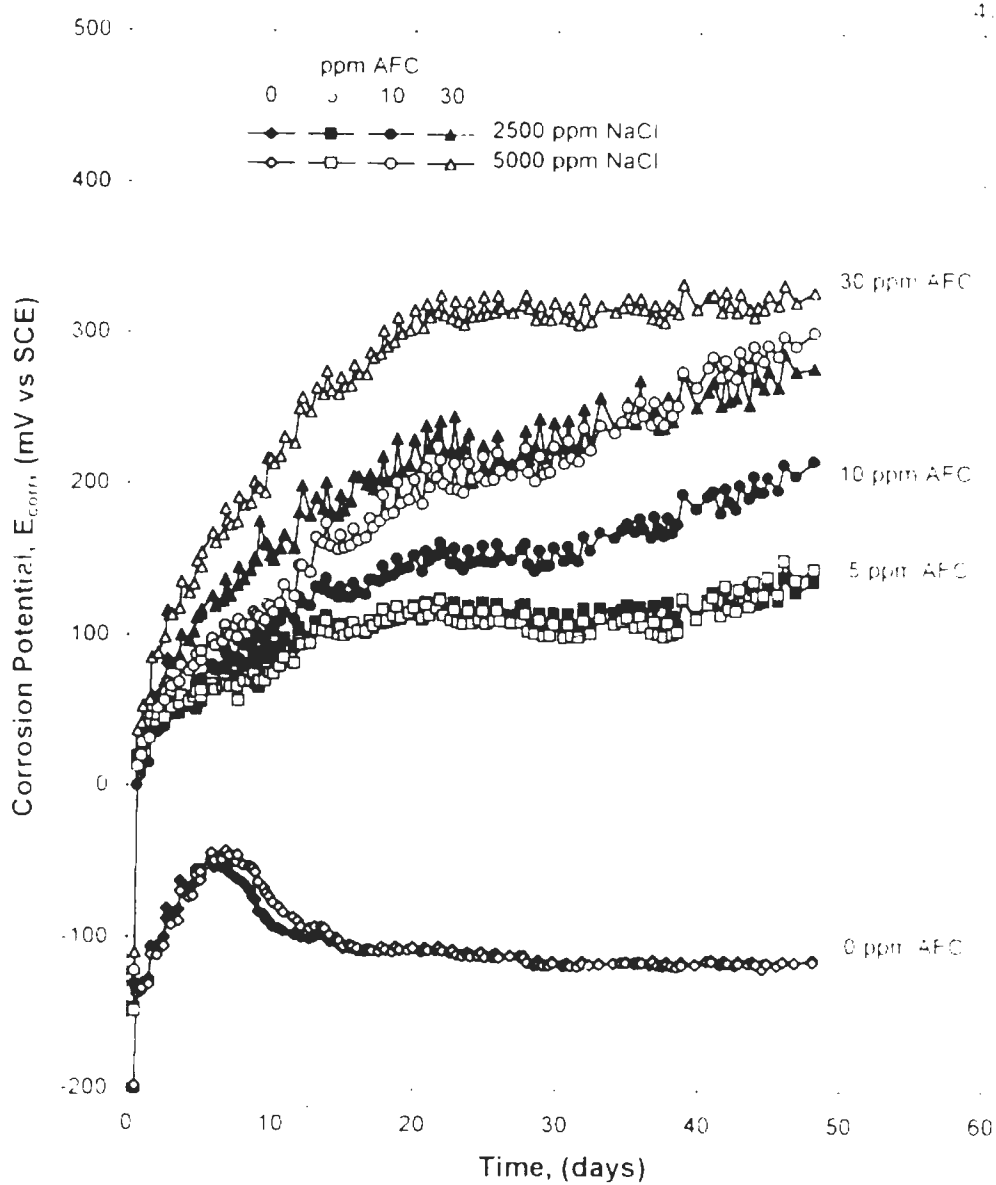


Figure 14 Effects of AFC and NaCl on corrosion potentials of 304SS exposed in simulated pool waters containing 50 ppm cyanuric acid. Each line mark represents one of various composition combinations in AFC and NaCl contents, as shown in the key.

potentials, which reached about 130 mV versus SCE. However, at 10 and 30 ppm AFC, the potentials in water with 5000 ppm NaCl were more noble than in the waters with 2500 ppm NaCl.

3) Effects of chlorine and chloride on corrosion potential, without cyanuric acid

The corrosion potentials versus exposure time were measured in chlorinated NaCl solutions, without cyanuric acid, but with variable AFC and NaCl contents. Figure 15 shows the corrosion potential movements during 50 day immersions without cyanuric acid. HOCl remarkably raised the corrosion potentials. For example, potential decline with 50 ppm cyanuric acid was not observed without cyanuric acid at 0 ppm AFC. The effects of NaCl concentration at 2500 and 5000 ppm were minor. At 0, 5 and 10 ppm AFC, the corrosion potentials in 5000 ppm NaCl solution showed slightly higher than in 2500 ppm NaCl solution. At 30 ppm AFC, the corrosion potentials showed slightly higher in 2500 ppm NaCl solution than in 5000 ppm NaCl solution. However, differences between 2500 ppm and 5000 ppm NaCl are probably within experimental reproducibility.

Figure 16 compares corrosion potentials in simulated pool waters with chlorinated NaCl solutions, at the same exposure length of 50 days. Clearly cyanuric acid suppresses the oxidizing ability of HOCl, especially at higher AFC contents. However, at the higher AFC contents, corrosion potentials were somewhat more noble at 5000 ppm NaCl than at 2500 ppm. That is, the cyanuric acid was

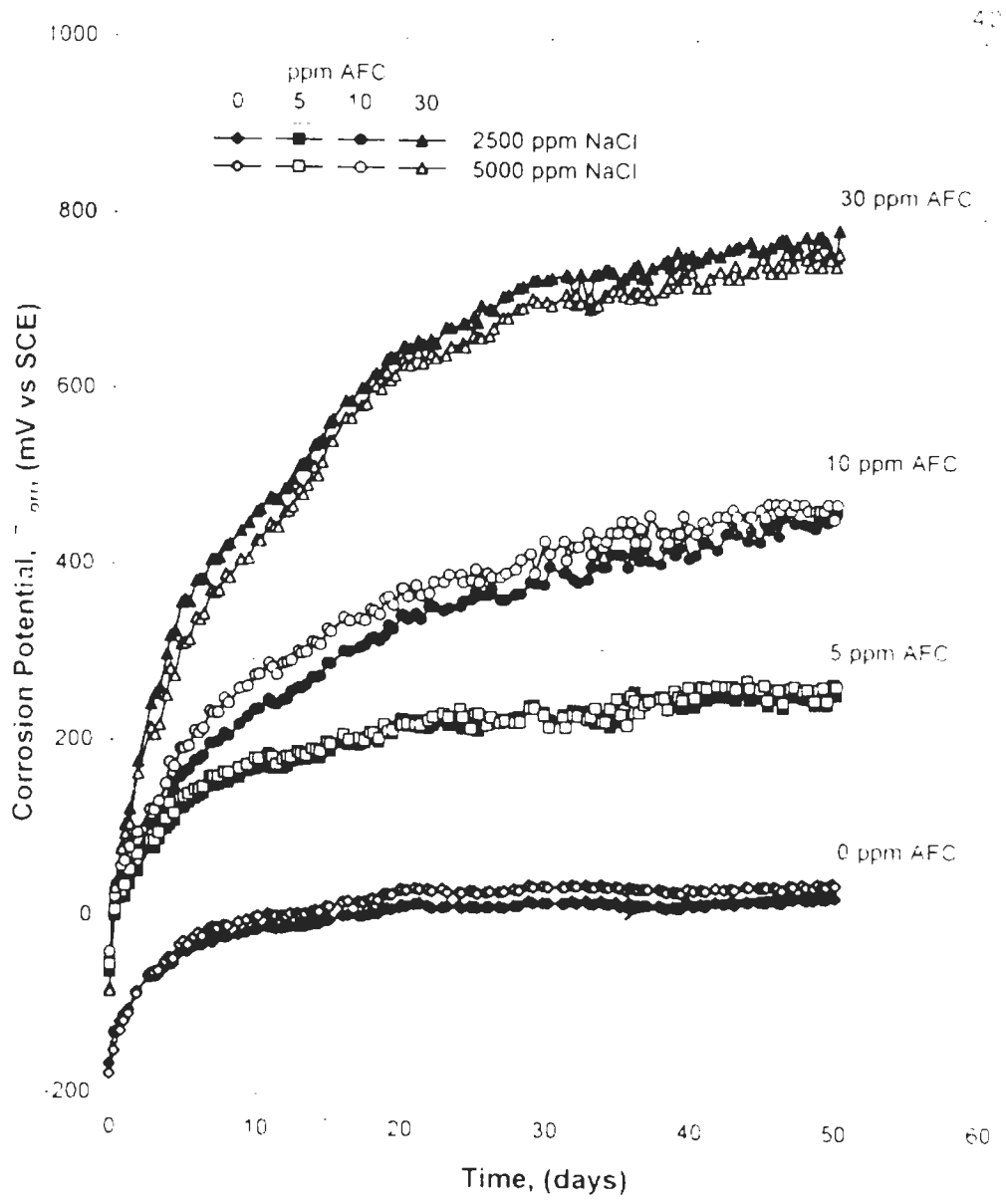


Figure 15. Effects of AFC and NaCl on corrosion potentials of 304SS exposed in chlorinated NaCl solutions. Each line mark represents one of various composition combinations in AFC and NaCl contents, as shown in the key.

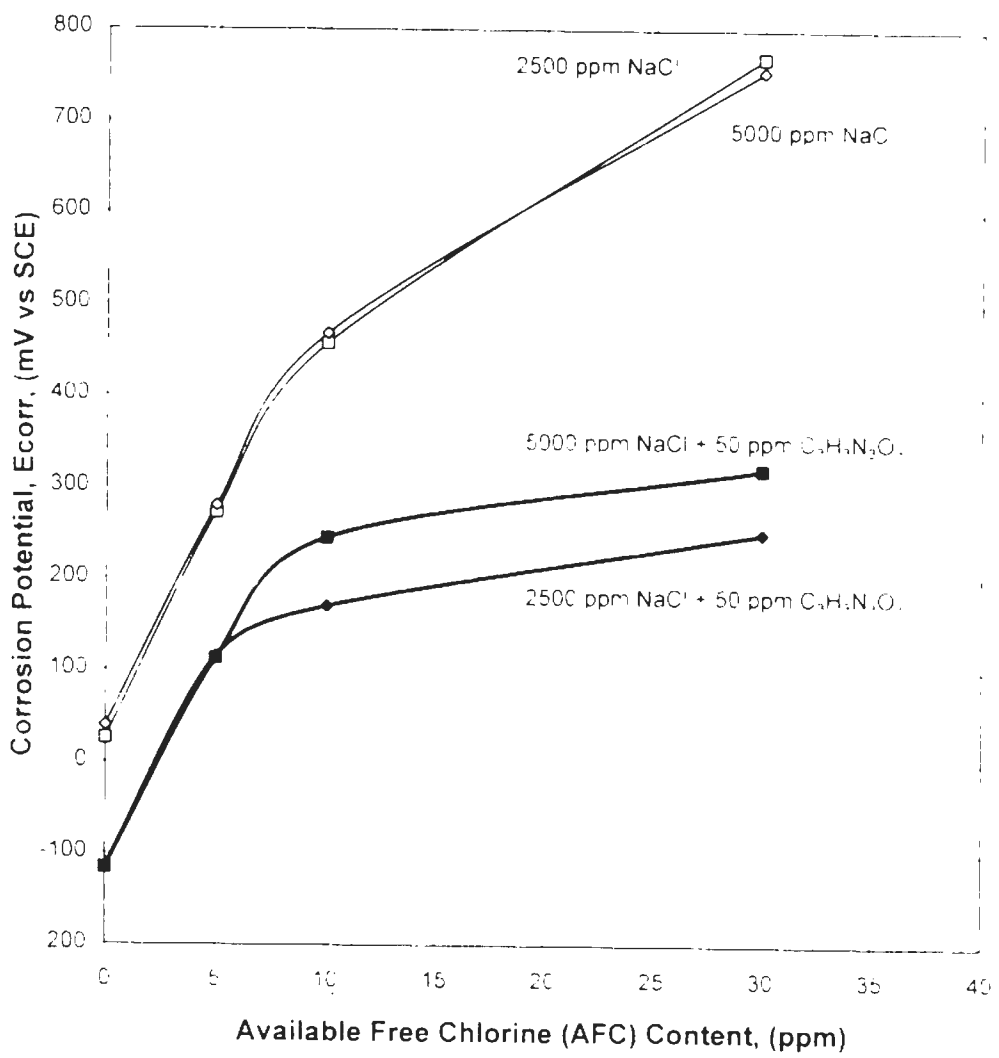


Figure 16 Comparison of average 50-day corrosion potentials in simulated pool waters and in similar chlorinated NaCl solutions

somewhat less effective at 5000 ppm than at 2500 ppm NaCl

Figure 17 shows corrosion potentials from 2-month continuous measurement in 10 ppm AFC + 5000 ppm NaCl solution. The corrosion potential moves in noble direction and reaches a steady state at about 400 mV versus SCE. After 14 days frequent potential spikes were present. The potential spikes showed a rapid drop followed by a slow rise, typified by Figure 18. Nevertheless, no observable pitting corrosion was present, even after 2 month exposure.

Figure 19 shows corrosion potentials measured from the filter tank containing a 10 ppm AFC + 5000 ppm NaCl solution. The potentials from widely separated points on inner tank surface are nearly identical. In first 4 days, the potentials moved up to about 50 mV versus SCE and moved down gradually thereafter. The tank potential in first 10 days was above measured protection potential (measured E_{prot} was about 20 mV vs SCE). After about 2 weeks, the potentials reached reasonably stable values below 0 mV. The lowest potential was measured around outlet tube area, where a crevice was formed by the rubber stopper. Evidence of crevice corrosion was observed after just 3-day exposure by accumulating of red ferric hydroxide corrosion products at the crevice mouth around the stopper. E_{prot} is shown on Figure 19 for comparison.

The upper curve in Figure 19 is the potential of a 35-cm² 304SS coupon specimen immersed in the solution without contacting the filter tank. The corrosion potentials of this coupon specimen were about 450 mV more noble than those of

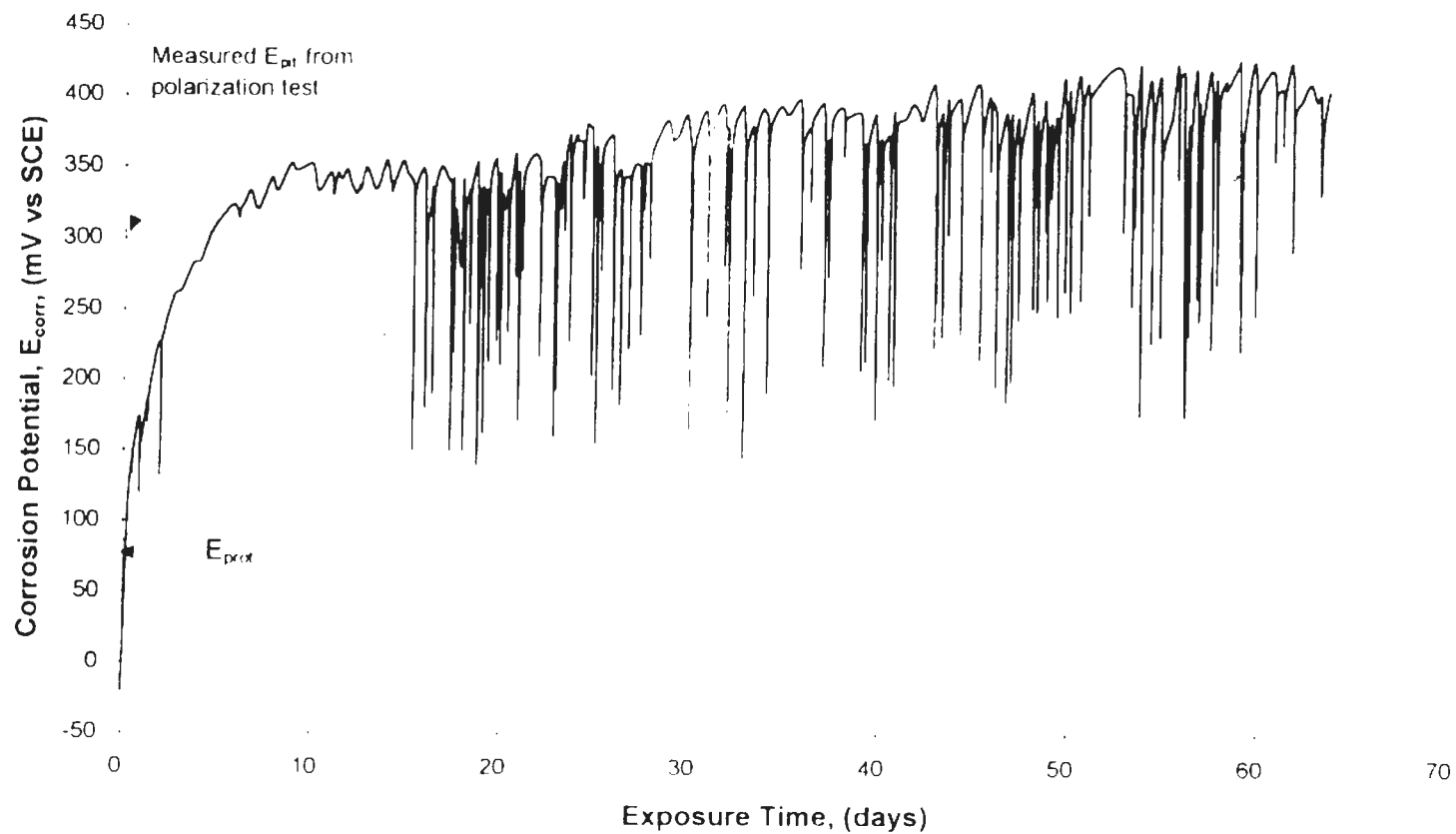


Figure 17. The corrosion potential of 304SS shifting in chlorinated water containing 10 ppm AFC + 5000 ppm NaCl. Each potential spike represents the procedure of pit initiation and repassivation.

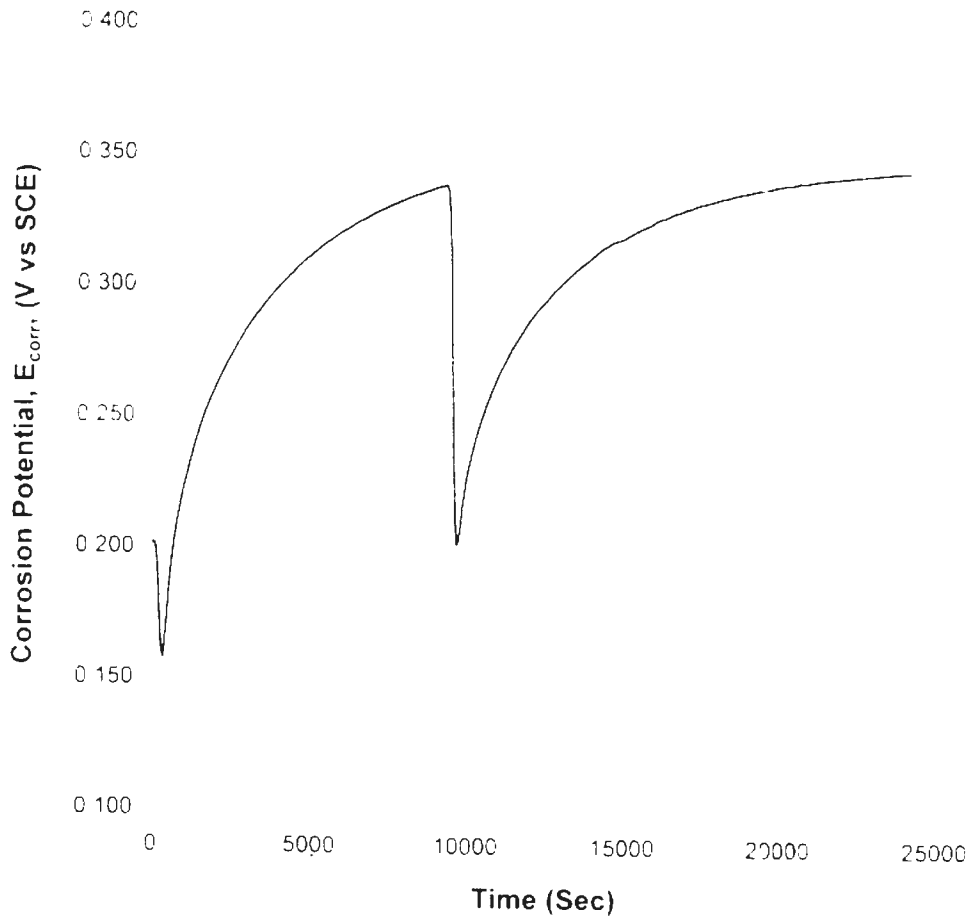


Figure 18. Portion of $E_{\text{corr}}-t$ curve showing pit initiation and repassivation. Pit initiation provides a rapid potential drop, while repassivation needs a slower procedure.

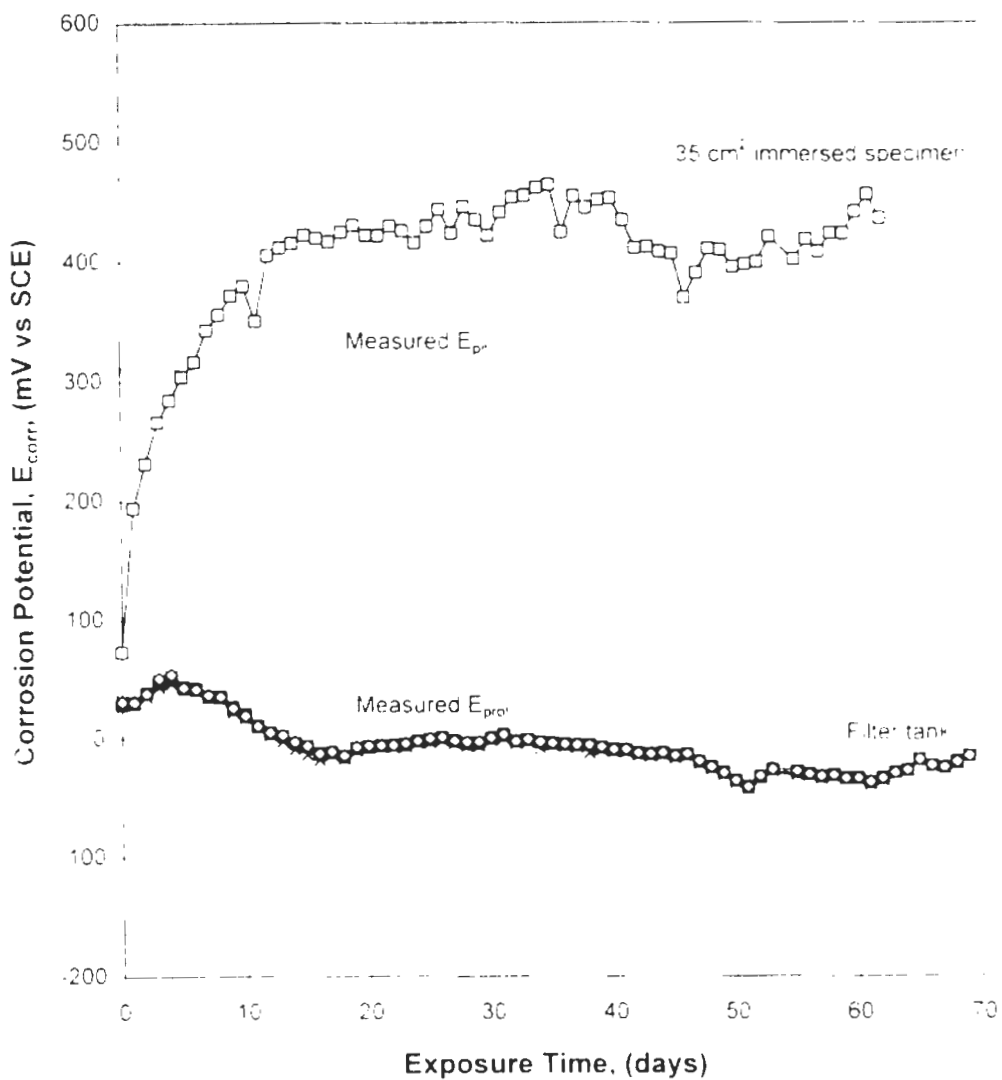


Figure 19. Corrosion potentials of filter tank showing very active during more than 2 month exposure in 10 ppm AFC+ 5000 ppm NaCl. The upper curve shows the corrosion potentials of immersed 304SS specimen, which is not contacted with filter tank.

the filter tank, and are comparable to the similar potentials in Figure 15 for 10 ppm AFC + 5000 ppm NaCl

4) Cyclic polarization behavior

Figure 20 shows cyclic polarization curves for 304SS in 2500 ppm NaCl solutions. With the addition of 10 ppm AFC, the pitting potential was shifted to more active values. Little effect of residual chlorine is observed on protection potential, but the observed E_{prot} had nearly same value as E_{corr} with presence of chlorine residual.

Figure 21 shows the cyclic polarization curves for the 304SS in simulated pool water with 2500 ppm NaCl + 50 ppm cyanuric acid. With the addition of 10 ppm AFC, the pitting potential was shifted to more active while the protection potential was not affected. With presence of cyanuric acid, the protection potential was well above the corrosion potential.

When chloride levels in the above solutions was raised to 5000 ppm NaCl, very similar behaviors were observed, as shown in Figure 22 and Figure 23. Without presence of chlorination, the pitting current after critical potential point showed rapid increase. However, the pitting current increased relatively slower, represented as shoulder in polarization curve, with presence of chlorination. Comparing Figures 20-23, some quantitative trends are summarized in Figure 24. Without AFC, the pitting potentials of 304SS were most noble, regardless of presence of cyanuric acid. With

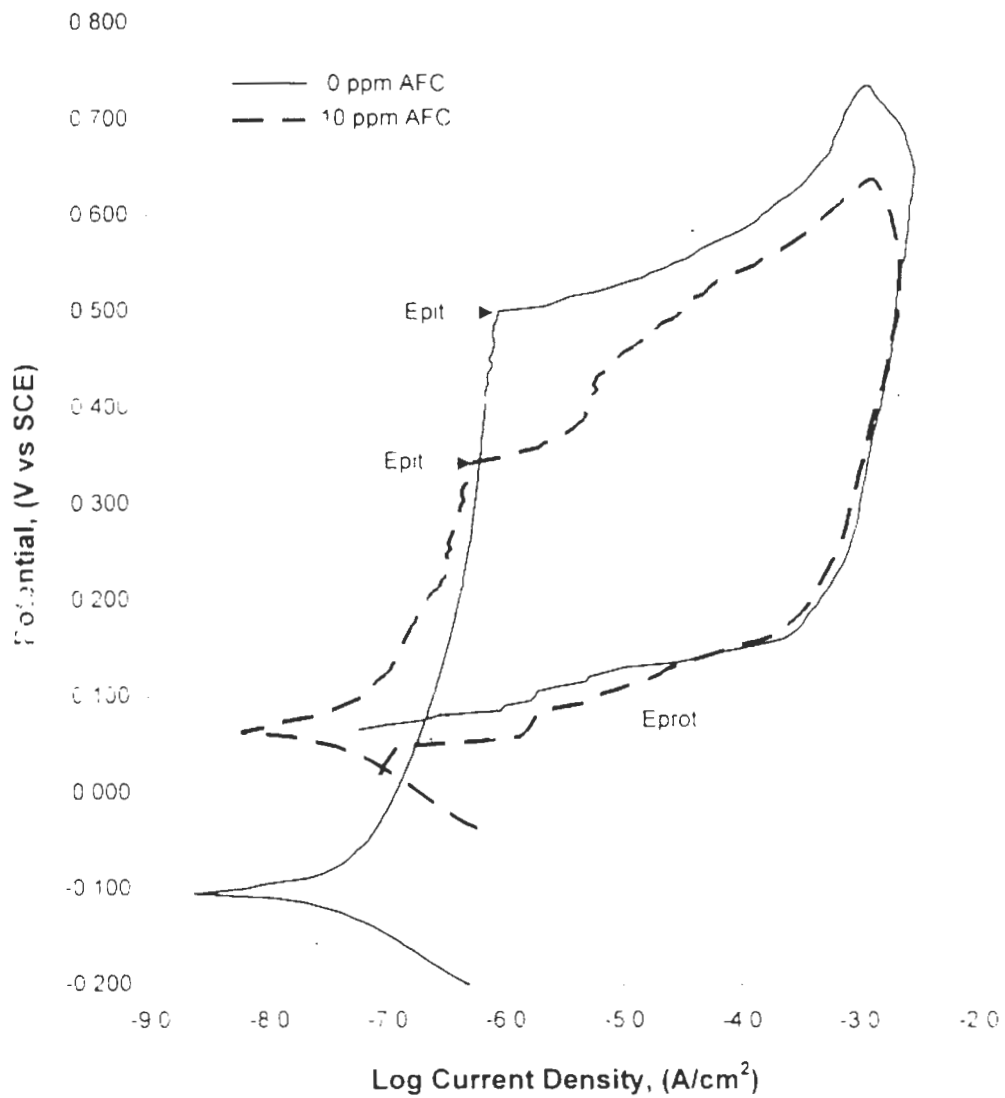


Figure 20. Chlorination effects on cyclic polarization behavior of Type 304 stainless steel in 2500 ppm NaCl solutions.

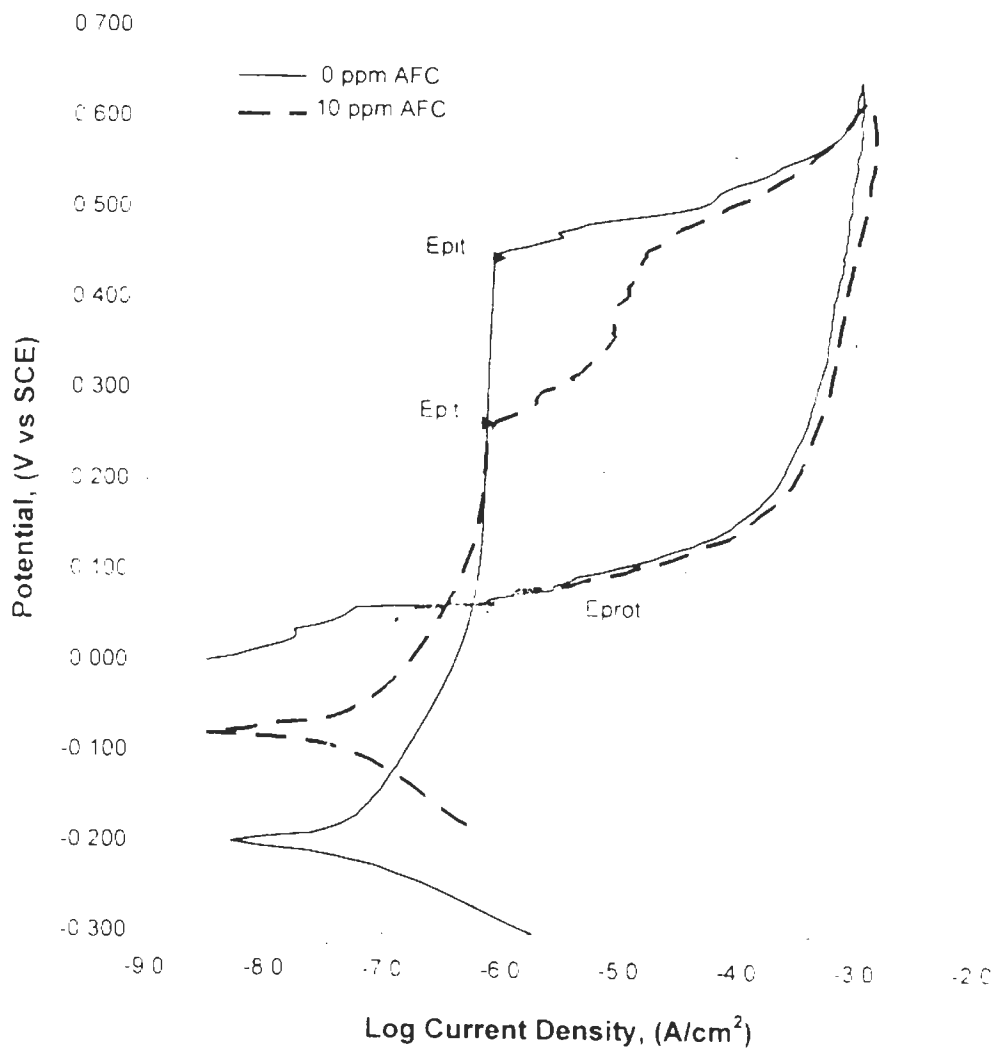


Figure 21. Chlorination effects on cyclic polarization behavior of Type 304 stainless steel in simulated pool waters, which contain 2500 ppm NaCl + 50 ppm cyanuric acid.

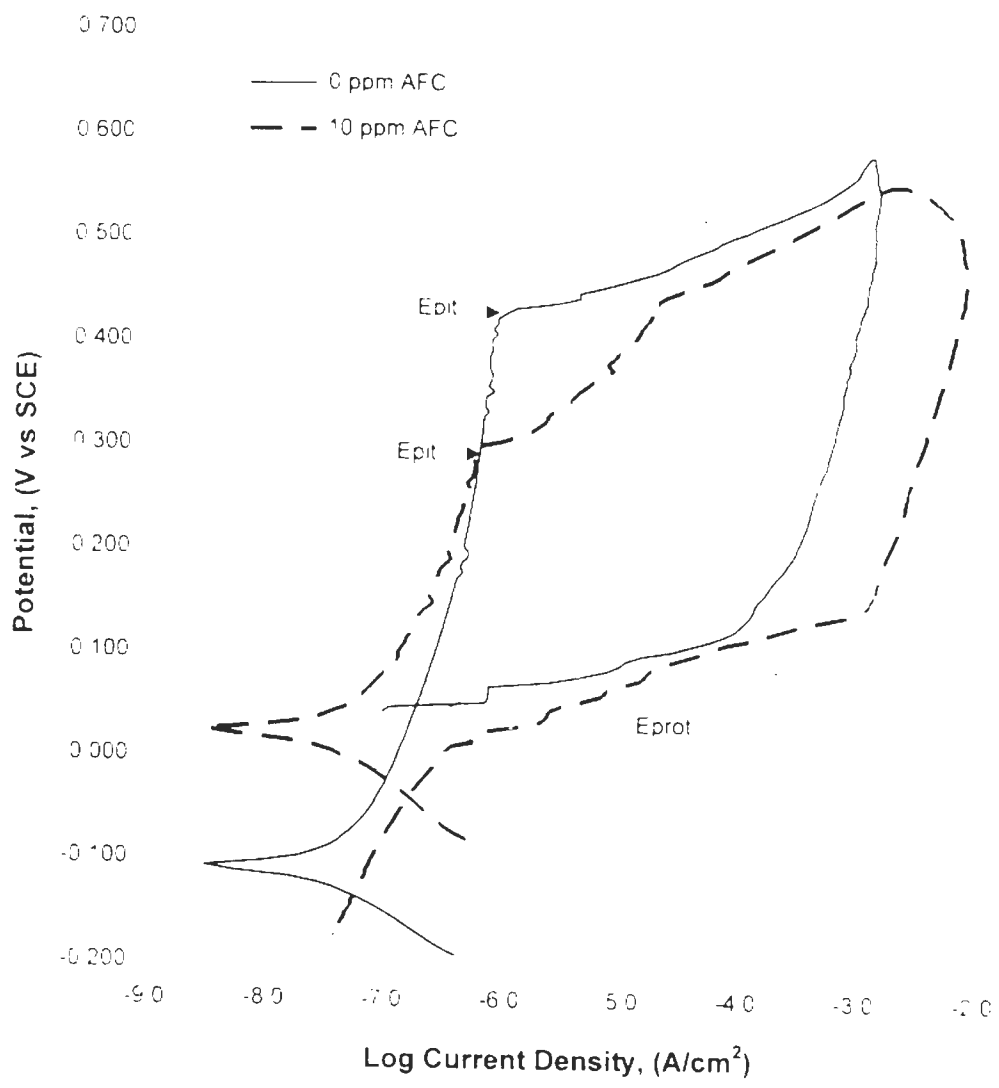


Figure 22. Chlorination effects on cyclic polarization behavior of Type 304 stainless steel in 5000 ppm NaCl solutions.

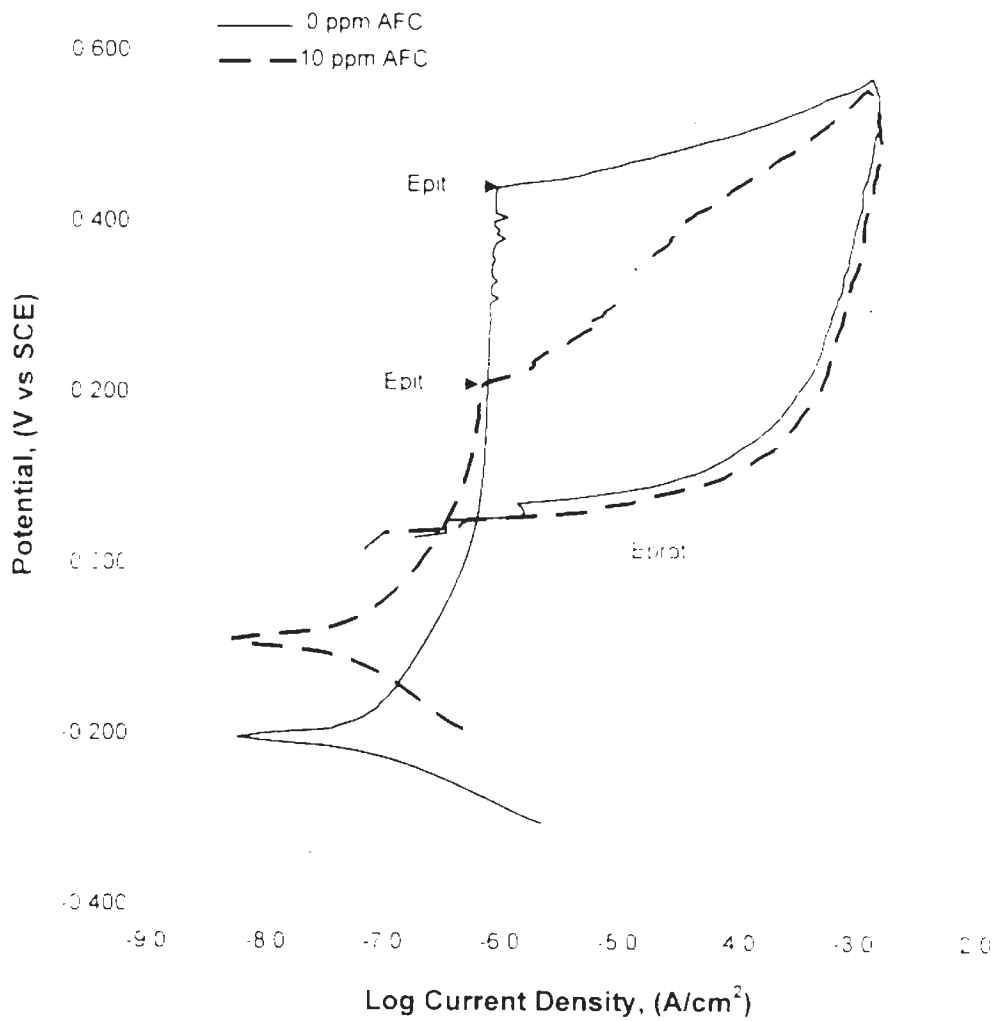


Figure 23. Chlorination effects on cyclic polarization behavior of Type 304 stainless steel in simulated pool waters, which contain 5000 ppm NaCl + 50 ppm cyanuric acid.

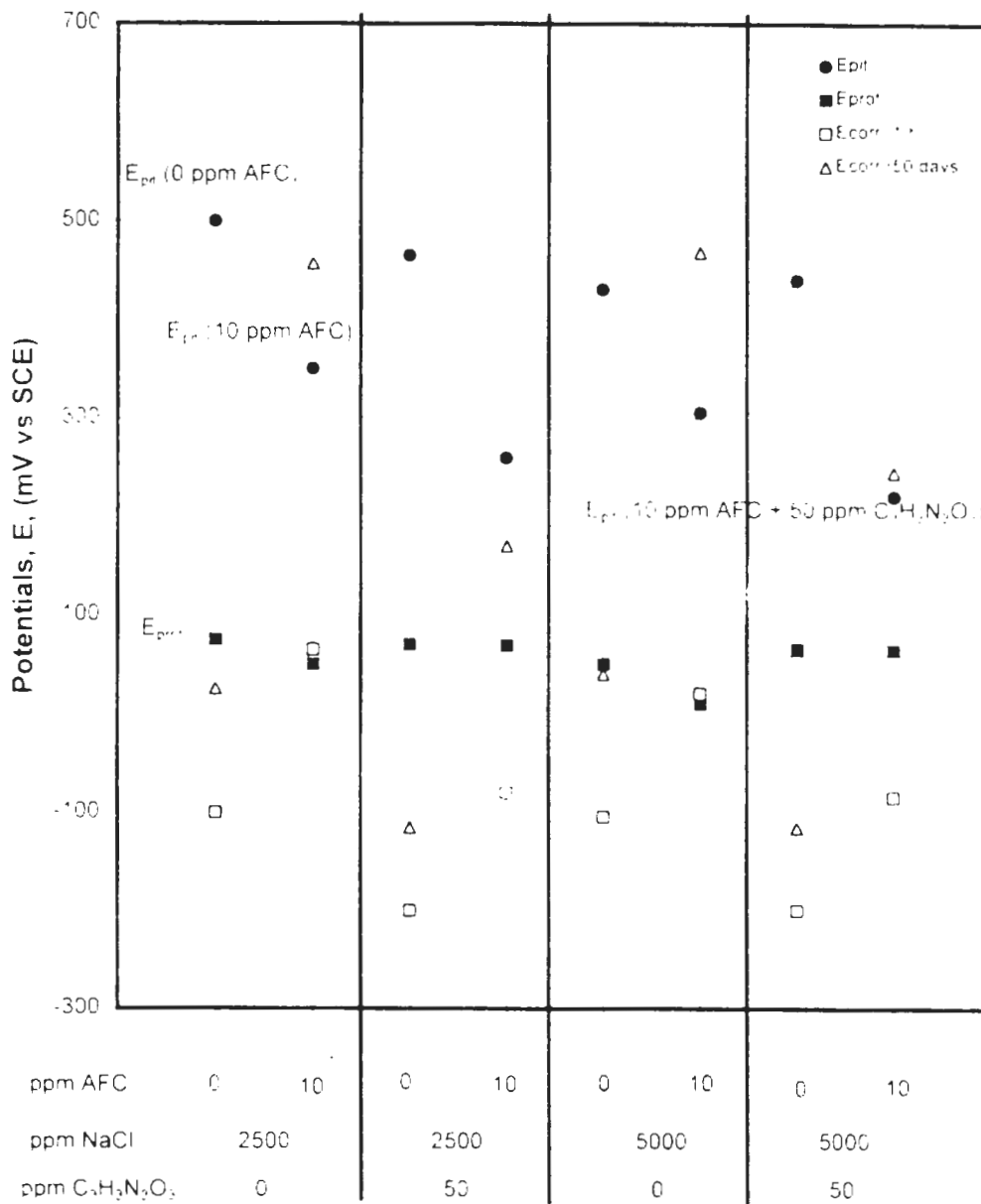


Figure 24. Combined plot with common vertical axis showing the measurements in E_{pit} , E_{prot} and E_{corr} in 4 groups of solution. The potential comparison suggests the effects of AFC, NaCl and $C_3H_3N_3O_3$ on pitting corrosion behavior.

HOCl, the pitting potentials were decreased remarkably, and still further decreased by cyanuric acid. NaCl did decrease the E_{pit} , but the decrease was minor, compared to that of chlorination. The protection potentials averaged around 80 mV versus SCE for all solutions. Effects of chlorination and cyanuric acid on E_{prot} were negligible in chloride solutions of 2500 and 5000 ppm.

Chlorination increased corrosion potentials, and E_{corr} could be increased up to higher than E_{prot} in chlorinated NaCl solutions. However, cyanuric acid retarded the increase on corrosion potential, but had no effect on protection potential. With $\text{C}_3\text{H}_3\text{N}_3\text{O}_3$, $E_{\text{corr}} < E_{\text{prot}}$ for 1 hour exposure, but $E_{\text{corr}} \gg E_{\text{prot}}$ after 50 day exposure. Therefore, with the presence of cyanuric acid in chlorinated waters, the susceptibility on crevice corrosion of 304SS increases gradually with increasing the exposure time.

CHAPTER V

DISCUSSION

Available free chlorine behaves as an oxidizer which is well evidenced by the observation of more noble corrosion potentials in chlorinated solutions. The addition of HOCl not only adds a cathodic reduction reaction, but also thickens the passive layer on metal surface. Thickening the passive layer is a kinetic process, which proceeds during the exposure time. This is evidenced by the observation of corrosion potential shifting in noble direction during exposure duration, as shown in Figure 7. The current results have shown that it takes days or weeks for corrosion potential to approach a plateau.

One previous study^[5] reports that addition of HOCl increases the pitting potential. It was explained by Lu and Duquette^[5] that addition of oxidizer created more stable passive film and increased the resistance to pitting initiation. However, the experiments in this investigation reveal the opposite: the addition of chlorine decreased the pitting potential.

Critical pitting potential E_{pit} becomes observable not only because of pit initiation, but also because of consequent pit propagation. However, it does not necessarily mean that there are no pit initiations before potential reaches E_{pit} . Those early pit initiations are not observable only because there is no successfully consequent pit propagation. For an active-passive metal or alloy, each early

initiation is related to individual film breakdown, and $E_{p,1}$ is related to systematic breakdown on passive film. Before the systematic breakdown, passive film is continuously thickened and dissolved, and experiences numerous breakdown and repassivation events since very beginning. Majority of early breakdown sites can be repassivated. However, a number of these early breakdown sites are only suppressed by some means, such as polarization, to keep from propagation; they become "dormant sites" and significantly affect the measurement of $E_{p,1}$. For convenience, the individual breakdown site will be noted as "micropit" through the rest of this discussion.

The concentration difference between the micropit and surrounding passive surface promotes galvanic corrosion. The metal substrate in bottom of a micropit is dissolved. When the active-passive metal or alloy is in neutral water, the cathodic reaction on surrounding surface is the reduction of oxygen, as shown in equation (6a)



Because of electrolytic attraction, the OH^- ions migrate into micropit. Dormant sites are rich in OH^- ions, and high pH inside micropits prevent pit growth. With presence of $HOCl$ in electrolyte, the cathodic reaction produces Cl^- , as shown in equation (8a)



Therefore, dormant sites become rich in Cl^- ions, which dramatically increases the

tendency of consequent pH growth

The presence of chloride provides a characteristic feature of dramatically decreasing the critical potential and increasing current at critical potential^[16]. This feature can be defined in a small region such as micropit, dormant site, or chloride island site. However, it is not well known how, from point of quantitative view, this locally electrochemical property change affects critical potential of entire body in macro. The macro potentials can be either largely or hardly influenced. Nevertheless, when corrosion potential of entire body reaches the critical potential of defined areas, $E_{\text{corr}} > E_{\text{pit}}$, pitting can occur at these defined area. This point has been well supported by the results shown in Figure 8^[29].

$E_{\text{corr}} > E_{\text{pit}}$ is a necessary, but not a sufficient condition for initiation of pits. The anodic dissolution due to a high chloride, low-pH microenvironment can be suppressed because unlimited mass transfer could unify the microenvironment into bulk environment, and repassivate the micropits. The further development in initiation must be supported by galvanic corrosion due to concentration differences between micropit and surrounding surface. The corrosion products from this further development collect at the pit mouth, which impedes easy escape of corrosion products but is sufficiently porous to permit migration of Cl^- into the micropit, thereby sustaining a high acid chloride concentration inside the micropits^[16]. Pitting initiates successfully from these micropit or dormant sites.

The HOCl concentration used in this investigation is relatively low compared

to the concentration used by Lu and Duquette¹⁹. Lower concentration of oxidizer leads to thinner of passive layer on surface, and the random film breakdown or formation of micropits is likely expected. The HOCl contributions to producing Cl⁻ in dormant sites is greater than to building a well passive film. At high HOCl concentration, a different scenario on passive film might lead to opposite results. However, Lu and Duquette did not provide the explanation in their report.

With cyanuric acid in chlorinated solution, pitting potential was measured about 60 mV more active than in solution without cyanuric acid. Because cyanuric acid reduces the oxidizing ability of AFC, the number of micropits repassivated by HOCl is decreased. Thus, more micropits can become dormant sites in presence of both AFC and cyanuric acid. Cyanuric acid further decreases the E_p in chlorinated solutions.

Unlike what is shown in Figure 8, Type 304 stainless steel did not pit in chlorinated solution during long term exposure. Only are initiation and ensuing repassivation of micropits observed, which are shown as potential spikes in E_{p-t} curve of Figure 17. A 35 cm² exposure surface area was used, and the maximum Cl⁻ concentration was 3035 ppm (5000 ppm NaCl) in this investigation. It seems that the insufficient surface area and low Cl⁻ ion concentration caused the absence for pitting. At low Cl⁻ concentration, migration and absorption of chloride are not adequate to maintain a high chloride, low-pH environment in micropits, the supplement of surface effect on E_{pit} becomes much more critical in pit initiation. The

crevice corrosion in filter tank occurring after 3-day exposure well supports the significance of surface effect on pitting. Even though there was no pitting corrosion observed on 304SS, but frequent potential spikes after $E_{corr} > E_{pit}$ can be interpreted as that the momentary pitting can not be continued without enough cathode area.

The observed chloride effect on pitting potential is consistent with the explanation in this investigation. Comparing with the results from Ergun and Turan,^[24] Leckie and Uhlig,^[25] and Johnson,^[26] this investigation have observed very similar chloride effects on pitting potentials, at low chloride concentration. However, the measured E_{pit} was independent of Cl^- ion concentrations, or even of test water compositions. This chloride effect on E_{pit} does not agree with the result shown in Figure 5^[24] (for carbon steel), but agrees with the observation shown in Figure 6^[24] (for Ni).

Once a pit becomes stable, the chemistry inside the pit is well removed from the bulk solution. The measurement of protection potential is significantly affected by the chemistry, especially Cl^- ions, inside the pit. During stable pit propagation, HOCl, cyanuric acid, and even chloride in bulk solution do not participate the reaction inside the pits. The accumulation of chloride in a stable pit is accomplished by penetration of Cl^- ions partially caused by concentration gradient, but mostly by electrolytic attraction. Therefore, protection potential is independent of bulk solution chemistry, as shown in Figure 24. However, HOCl can bring the potential of the surrounding surface up to the value near or higher than protection potential, which

can accelerate the rate of pitting and crevice corrosion. Severe crevice corrosion in filter tank has been observed in the crevices formed by outlet tubes and the rubber stopper. Cyanuric acid retards oxidizing ability of HOCl, which could keep corrosion potential below the protection potential only for short exposure, but not for long exposure.

In Figure 14, the corrosion potential of filter tank showed higher than measured protection potential E_{prot} in first 10 days of immersion. This is a perfect example of how the protection potential varies with the change of electrochemical properties inside crevices or pits. The corrosion potential of filter body was still above the protection potential, only the protection potential decreased along with the lasting of crevice corrosion. It is a consistent observation that was evidenced by the crevice corrosion in the tank. The crevice corrosion started right after the beginning of immersion, and continued all way through the immersion length, even though the corrosion potential was below the measured E_{prot} .

The cyclic polarization curves obtained in chlorinated solutions showed a pitting current shoulder in Figures 20 - 23. This behavior can be explained as: In the early stage of pit propagation, the reduction of HOCl



increases Cl^- ions inside the pits, which accelerates the propagation rate. After the pit is occluded, the anodic dissolution rate decreases with consumption of HOCl and decrease of Cl^- ion concentration.

CHAPTER VI

CONCLUSION

The following conclusions can be drawn from the experimental results of this investigation

- 1 HOCl resulting from chlorination shifted the corrosion potential of Type 304 stainless steel in the noble direction. Chlorination thickens the passive layer on 304SS surface with increasing exposure duration. It takes days or even weeks to reach the stable passivation.
- 2 Chlorination decreased the pitting potential, or increased pitting susceptibility of Type 304 stainless steel in simulated swimming pool water. Chlorination enhances the absorption of Cl⁻ inside dormant sites and micropits.
- 3 After 2 week exposure, initiation and ensuing repassivation of micropits were observed on Type 304 stainless steel in chlorinated NaCl solution. The events were recorded as a rapid potential drop followed by slower rise, or the potential spikes in E_{corr} -t curve. The momentary pitting events could not continue because of insufficient cathode surface area.

CHAPTER VI

CONCLUSION

The following conclusions can be drawn from the experimental results of this investigation

- 1 HOCl resulting from chlorination shifted the corrosion potential of Type 304 stainless steel in the noble direction. Chlorination thickens the passive layer on 304SS surface with increasing exposure duration. It takes days or even weeks to reach the stable passivation.
- 2 Chlorination decreased the pitting potential, or increased pitting susceptibility of Type 304 stainless steel in simulated swimming pool water. Chlorination enhances the absorption of Cl⁻ inside dormant sites and micropits.
- 3 After 2 week exposure, initiation and ensuing repassivation of micropits were observed on Type 304 stainless steel in chlorinated NaCl solution. The events were recorded as a rapid potential drop followed by slower rise, or the potential spikes in E_{corr} -t curve. The momentary pitting events could not continue because of insufficient cathode surface area.

4 No remarkable pitting corrosion was observed on Type 304 stainless steel during 2 month exposure in chlorinated solutions. Insufficient cathode area and low Cl concentrations (<5000 ppm NaCl) could not convert momentary pitting into stable pitting.

5 Chlorination did not affect the protection potential significantly. But chlorination brought the corrosion potential up to a value near or even higher than protection potential, then accelerated crevice corrosion. Severe crevice corrosion was observed with the crevice geometry and large surrounding area in chlorinated NaCl solution.

6 Chloride decreased E_{p1} , but did not affect protection potential. Chloride effect on corrosion potential in chlorinated NaCl solution was negligible, but higher chloride content increased E_{corr} , when 10 and 30 ppm AFC were present in simulated pool water.

7 Cyanuric acid retarded the increase of corrosion potential of 304SS in simulated pool water in the presence of HOCl. Cyanuric acid did not affect protection potential. At large times E_{corr} was able to exceed E_{prot} even with cyanuric acid, and susceptibility to crevice corrosion increased.

REFERENCES

- 1) G. C. White. **The Handbook of Chlorination and Alternative Disinfectants**. Third edition, pp. 184-191, Van Nostrand Reinhold, New York, 1992
- 2) P. D. Goodman, "Effect of Chlorination on Materials for Sea Water Cooling Systems: a Review of Chemical Reactions", **Br. Corros. J.**, Vol. 22, No. 1, pp. 56-62, 1987
- 3) **Pool & Spa Water Chemistry: testing and treatment guide with tables**. Taylor Technologies, Inc., Sparks, MD, 1990
- 4) E. D. Robinton and E. W. Mood, "An Evaluation of The Inhibitory Influence of Cyanuric Acid Upon Swimming Pool Disinfection", Vol. 57, No. 6, pp. 301-310, **American Journal of Public Health**, 1967
- 5) **Basic Pool and Spa Technology**, D. S. Rennell ed., National Spa and Pool Institute, Arlington, Va., pp. 390, c1989
- 6) M. Pourbaix, **Atlas of Electrochemical Equilibria in Aqueous Solutions**, pp. 591, NACE, Houston, 1974
- 7) M. B. Ives, Y. C. Lu and J. L. Luo, "Cathodic Reactions Involved in Metallic Corrosion in Chlorinated Saline Environments" **Corrosion Science**, Vol. 32, No. 1, pp. 91-102, 1991
- 8) H. H. Lu and D. J. Duquette, "The Effect of Dissolved Chlorine on The Pitting Behavior of 304L Stainless Steel in a 0.5 N NaCl Solution", **Corrosion**, Vol. 46, No. 12, pp. 994-1001, TX, 1990.
- 9) S. M. Sharland, C. M. Bishop, P. H. Balkwill and J. Stewart, "The Initiation of Localized Corrosion: A Process Governed by a Strange Attractor?", **Advances in Localized Corrosion**, NACE-9, H. S. Isaacs, U. Bertocci, J. Kruger, and S. Smialowska, eds., NACE, Houston, TX, pp. 109-115, 1987
- 10) Z. Szklarska-Smialowska, "Pitting Initiation", **Advances in Localized Corrosion**, NACE-9, H. S. Isaacs, U. Bertocci, J. Kruger, and S. Smialowska, eds., NACE, Houston, TX, pp. 41-45, 1987

- 11) B. E. Wilde, "Chloride ion Adsorption and Pit Initiation on Stainless Steels in Neutral Media", **Passivity and Its Breakdown in Iron Base Alloys**, R. Staehle, H. Okada eds., NACE, Houston, pp. 129, 1976
- 12) M. Janik-Czachor, A. Szummer and Z. Szklarska-Smialowska, "Electron Microprobe Investigation of Processes Leading to The Nucleation of Pits" **Corrosion Science**, Vol. 15, pp. 775-778, 1975
- 13) T. Okado, "Halide Nuclei Theory of Pit Initiation in Passive Metals" **J. Electrochem. Soc.**, Vol. 131, No. 2, pp. 241-246, 1984
- 14) S. Szklarska-Smialowska, "The Pitting of Iron-Chromium-Nickel alloys" **Localized Corrosion**, NACE-3, R. Staehle, B. Brown, J. Kruger, A. Agrawal eds., NACE Houston TX, pp. 312-341, 1974
- 15) G. R. Wallwork and B. Harris, "Localized Corrosion in Mild Steel", **Localized Corrosion**, NACE-3, R. Staehle, B. Brown, J. Kruger, A. Agrawal, eds., NACE Houston TX, pp. 292-304, 1974
- 16) D. A. Jones, **Principles and Prevention of Corrosion**, Macmillan Publ., New York, NY, pp. 208-215, 1992
- 17) S. Szklarska-Smialowska, "The Pitting of Iron-Chromium-Nickel alloys" **Localized Corrosion**, NACE-3, R. Staehle, B. Brown, J. Kruger, A. Agrawal, eds., NACE Houston, TX, pp. 312-341, 1974
- 18) D. A. Jones, **Principles and Prevention of Corrosion**, Macmillan Publ., New York, NY, pp. 213-219, 1992
- 19) J. A. Beavers and N. G. Thompson, "Effect of Pit Wall Reactivity on Pit Propagation in Carbon Steel" **Corrosion**, NACE, Vol. 43, No. 3, pp. 185-188, 1987
- 20) Z. Szklarska-Smialowska, **Pitting Corrosion of Metals**, NACE Publ., Houston TX, pp. 113-125, 1986
- 21) D. A. Jones, **Principles and Prevention of Corrosion**, Macmillan Publ., New York, NY, pp. 218, 1992
- 22) B. E. Wilde, "On Pitting and Protection Potentials: Their Use and Possible Misuses for Predicting Localized Corrosion Resistance of Stainless Alloys in Halide Media", **Localized Corrosion**, NACE-3, R. Staehle, B. Brown, J. Kruger, A.

Agrawal, eds., NACE, Houston, TX, pp 342-350, 1974

23) Z. Szklarska-Smialowska **Pitting Corrosion of Metals** NACE Publ., Houston TX, pp 202-212, 1986

24) M. Ergun and A. Y. Turan, "Pitting Potential and Protection Potential of Carbon Steel for Chloride Ion and The Effectiveness of Different Inhibiting Anions" **Corrosion Science**, Vol. 32, No. 10, pp. 1137-1142, 1991

25) H. P. Leckie and H. H. Uhlig, "Environmental Factors Affecting the Critical Potential for Pitting in 18-8 Stainless Steel" **J. Electrochem. Soc.**, Vol. 113, No. 12, pp. 1262-1267, 1966

26) M. J. Johnson, "Relative Critical Potentials for Pitting Corrosion of Some Stainless Steels" **Localized Corrosion—Cause of Metal Failure** ASTM STP 516 American Society for Testing and Materials, 1972, pp 262-272

27) G. Sussek and M. Kesten, "Eine Charakterisierung Der Lochfrabkorrosion Des Nickels—I. Die Bestimmung Der Lochfrabpotentiale in neutralen und Alkalischen Losungen" **Corrosion Science**, Vol. 15, No. 4, pp. 225-239, 1991

28) D. A. Jones **Principles and Prevention of Corrosion**, Macmillan Publ., New York, NY, pp 137-138, 1992

29) B. E. Wilde and E. Williams, "On the Correspondence between electrochemical and Chemical Accelerated Pitting Corrosion Tests", **J. Electrochem. Soc.**, Vol. 117, No. 5, pp 775, 1970

30) R. Guo, S. C. Srivastava and M. B. Ives, "Pitting Corrosion Behavior of UNS N08904 Stainless Steel in a Chloride/Sulfate Solution", **Corrosion**, NACE, Vol. 45, No. 11, pp 874-882, 1989.

31) Y. C. Lu, J. L. Luo and M. B. Ives, "The Influence of Chlorination of Saline Environments on Localized Corrosion of Stainless Steels", **ISIJ International**, Vol. 31, No. 2, pp 210-215, 1991

32) S. Magaino, A. Kawaguchi, A. Hirata and T. Osaka, "Spectrum analysis of corrosion potential fluctuations for localized corrosion of type 304 stainless steel" **J. Electrochem. Soc.**, Vol. 134, No. 12, pp 2993-2997, 1987

33) G. Daufin, J. Pagetti, J. P. Labbe and F. Michel, "Pitting Initiation on Stainless

Steels. Electrochemical and Micrographic Aspects", **Corrosion**, NACE, Vol. 41, No. 9, pp. 533-539, 1985

34) T. Yoshii, M. Nishikawa and T. Mackita, "Effect of The Residual Chlorine Behavior of The Corrosivity on Stainless Steels". Technical Report in Nisshin Steel Co., No. 42, pp. 25-39, Tokyo, Japan, July 1980.

35) G. C. White, **The Handbook of Chlorination and Alternative Disinfectants** Third edition, pp. 259-261, Van Nostrand Reinhold, New York, 1992

36) ASTM Standard, "Standard Reference Test methods for Making Potentiostatic and Potentiodynamic Anodic polarization Measurements" Designation G 5 **Annual Book of ASTM Standards**, Vol. 3.02, 1990

37) ASTM Standard, "Conducting Cyclic Potentiodynamic Polarization Measurements for Localized Corrosion" Designation G 61, **Annual Book of ASTM Standards**, Vol. 3.02, 1990